POLITECNICO DI MILANO

Scuola di Ingegneria Industriale e dell'Informazione

Master of Science in Automation and Control Engineering

ATTITUDE AND POSITION CONTROL FOR A SMALL SCALE QUAD-TILTROTOR

Supervisor: Prof. Marco Lovera

Master thesis by:
Ehsan Fathi
Student ID: 817746

Academic Year 2015 - 2016

To my family

Acknowledgements

I would like to express my special appreciation to my advisor Prof. Marco Lovera for sharing valuable guidance and encouragement.

Special thanks to my parents for their support and attention throughout writing this Thesis and in my whole life in general.

Abstract

Small scale unmanned aerial vehicles (UAVs) are getting very popular among people and research communities due to their different applications such as traffic monitoring, exploration of disasters (fire, earthquake, flood), military purposes, etc. Although numerous research has been conducted so far, conventional quad-rotors still suffer from limited mobility and maneuverability. Having four independent control inputs (four propeller spinning velocities) versus six degrees of freedom (position and orientation) in space makes this kind of UAVs not fully controllable. In most of cases, position (X,Y,Z) and yaw angle (ψ) are considered as outputs, then pitch and roll angles cannot be controlled. Eventually, they cannot track an arbitrary trajectory in space, they cannot stay in a desired position and orientation, they cannot remain in a predefined altitude and attitude in presence of disturbances such as wind, they are not able to land on ramp surfaces, etc. In this thesis we overcome the aforementioned problems by designing attitude and position controllers for a novel overactuated quad-rotor which has four extra motors actuating on the propellers tilting angles. To achieve the aim of this thesis, first, thanks to Newton-Euler formulation a comprehensive and accurate mathematical model is developed and then it is linearized around the hovering state. Second, an adjustable parameter β ($0 \leqslant \beta \leqslant 1$) is introduced which enables us to choose a desired mode of operation between conventional quad-rotor ($\beta = 0$) and full quad-tiltrotor ($\beta = 1$) dynamically. Finally, two optimal controllers (LQ and H_∞) are developed to control the position and attitude of the quad-tiltrotor in a desired state. These controllers are designed not only to stabilize the system, but also to ensure that the outputs track the reference inputs in presence of disturbances. Finally, the results of several simulations are reported to illustrate the capabilities of the proposed novel UAV design.

Contents

Chapter 1

Introduction

The interest of mankind for aerial vehicles in general has always been flourishing, and in the twentieth century the aircraft industry has seen its birth and boost due to military employment first and civilian transport then [1]. The concept of Unmanned Aerial Vehicles (UAVs), or drones, was born quite early in the twentieth century: as far back as in 1915 Nikola Tesla described an armed, pilotless aircraft designed to defend the United States [2]. The development of UAV technology has regarded largely military purposes, but lately a lot of civilian applications have become established as well. The main applications are intelligence gathering, surveillance, platooning, as well as climate and pollution monitoring, rescuing operations, pipeline inspection [3]. The success of this technology relies in replacing the human presence when navigation and maneuver in adverse or uneasily reachable environments is needed.
The small-scale UAVs can be grouped into three categories: rotorcraft, fixed-wing and flapping-wing. In this thesis we exclude fixed-wing and flapping-wing UAVs and focus on rotorcraft UAV. Among different types of rotorcraft UAVs, quadrotor is more popular and many control approaches have been developed for it. Currently, there are various commercial and experimental quad-rotors of various sizes available but these UAVs are an underactuated system with six outputs and four inputs which only the Cartesian position and yaw angle with respect to an inertial frame can be independently controlled. Over the last decades, for an effective and robust flight performance, many modeling approaches have been presented and various control methods proposed such as PID controller and LQ controller [4], full-state backstepping technique based on Lyapunov stability theory [5], backstepping sliding mode control [6], feedback linearization control [7], feedback linearization with a high-order sliding mode observer [8], Robust adaptive fuzzy control [9], nonlinear H-infinity controller with backstepping [10] and so on.

Despite of all the researches have been conducted so far, conventional quadrotors still suffer from limited maneuverability. Having four independent control

inputs versus six degrees of freedom make them not fully controllable.

One of the limiting factors which prevents further implementation of the quad-rotor system into applications is presented in [11], that is the way quad-rotor moves. Indeed, it needs to tilt along the desired direction of motion by doing this it can have necessary acceleration towards that direction as well as tilting has the undesired effect of moving the onboard cameras' direction of view. This becomes an issue for surveillance and other vision based tasks. Besides the aforementioned issue, conventional quad-rotors have other problems which some of them are as follows: they are not able to track arbitrary trajectories for their body position and orientation, they cannot remain in a predefined altitude and attitude in presence of disturbances such as wind, they are not able to land on ramp surfaces, etc.

These problems motivated us to use a novel model of UAVs to overcome these limitations.

1.1 Literature review

In this section we investigate different types of UAVs and study their advantageous over the conventional quad-rotors and then a novel model is used for which a controller will be developed in Section 3.

A novel trirotor helicopter has been presented in [13]. The helicopter is composed of three rotors with constant pitch propellers; two fixed rotors turning in opposite directions and one rotor that can be tilted to control the yaw displacement as shown in Figure 1.1. Since the two front rotors rotate in opposite directions, the generated reaction torque is almost zero. The tail rotor can be tilted using a servomechanism in order to produce a yaw torque. The angular velocity of the two main rotors can be adjusted to produce the main thrust as well as the roll torque. The roll torque is obtained as a function of the angular speed difference of the two main rotors. Finally, the pitch torque is obtained by varying the angular speed of the tail rotor.

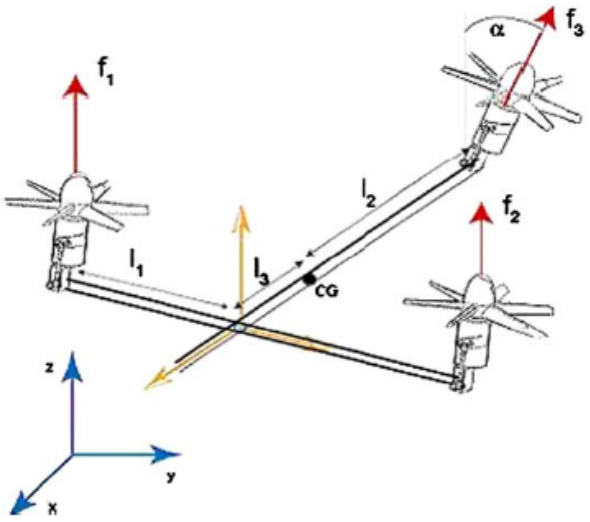

Figure 1.1: Trirotor configuration

It is clear that one of the advantages of this trirotor with respect to conventional quadrotors is that it requires one motor less which can lead to a reduction in weight, volume and energy consumption.

A triple tilting rotor mini-UAV has been presented in [14]. This mini-UAV has three rotors located at the same distance from its center of gravity. This structural feature (symmetry) allows to provide a symmetric lift contribution for the vehicle, improving its stability and payload capability.

The proposed vehicle provides a reliable maneuverability despite the reduced number of rotors. The authors designed a controller to control the altitude and attitude of this triple tilting rotor mini-UAV. Figure 1.2 shows the free-body scheme and how propellers are tilted.

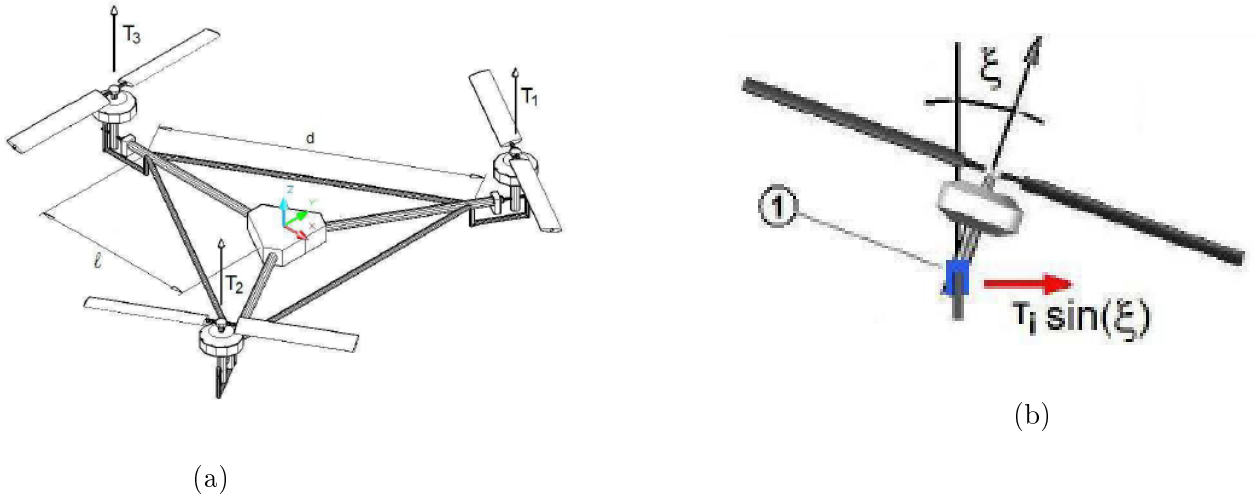

(a) (b)

Figure 1.2: (a) Rotorcraft free-body scheme (b) Tilting mechanism

In [15] a new kind of quad-rotor helicopter with 4 propellers is proposed, 3 of which are horizontally mounted to control its pitch and roll rotation while the last one is vertically mounted to control its yaw rotation as shown in Figure 1.3. Therefore, it has the advantage of classical helicopters in yaw motion control and also has the advantage of quad-rotors in pitch and roll motion control [15].

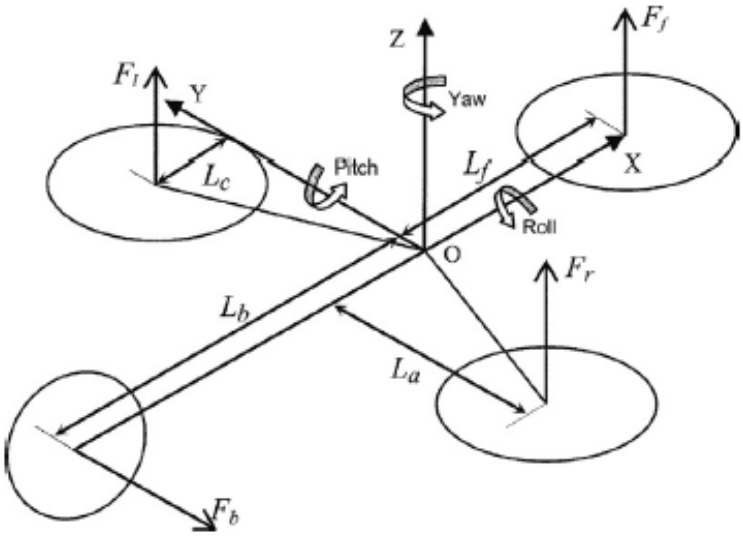

Figure 1.3: Quad-rotor helicopter configuration

A tilt-roll quad-rotor UAV has been designed in [16] which can tilt each rotor independently along the X and Y axes. In this UAV, unlike in the conventional one, the rotors are able to rotate around pitch and roll angles. The required force is generated not by tilting the body itself, but by tilting the required rotors.

Therefore, in comparison with conventional quad-rotors, it adds 8 additional control inputs to the system and totally provides 12 control inputs (see Figure 1.4). Although these additional control inputs make the system mechanically more complex, it brings various advantages. This design eliminates the need of tilting the airframe, and it suggests better performance with respect to conventional quad-rotor design [16].

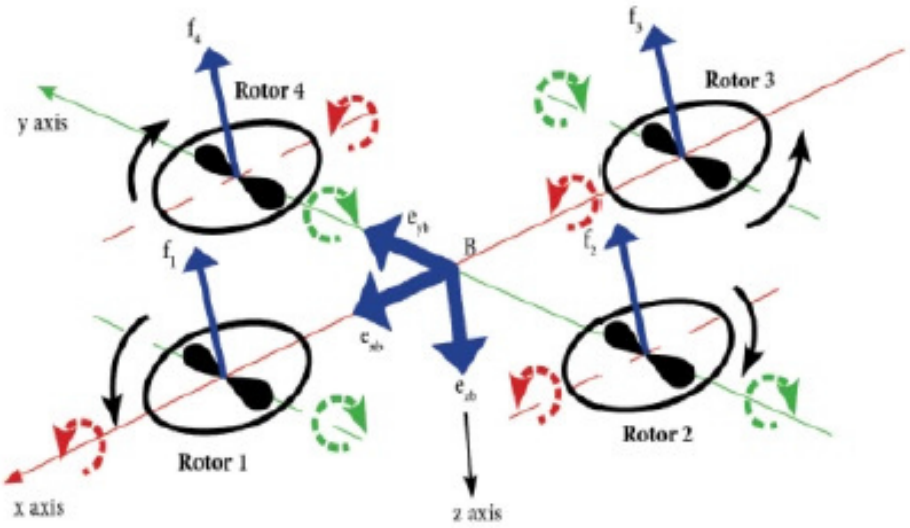

Figure 1.4: Free body diagram of tilt-roll rotor quadrotor

In [17], they presented a new configuration of a multirotor aircraft having eight rotors. This UAV is able to perform vertical take-off and landing, hovering and translational flight. The main advantage of the proposed configuration is that the attitude dynamics is decoupled from the translational dynamics.

Moreover, this configuration allows to maintain to the mini helicopter stable using the main rotors (inner rotors) and perform lateral displacements only using the auxiliary rotors (lateral rotors)(see Figure 1.5).

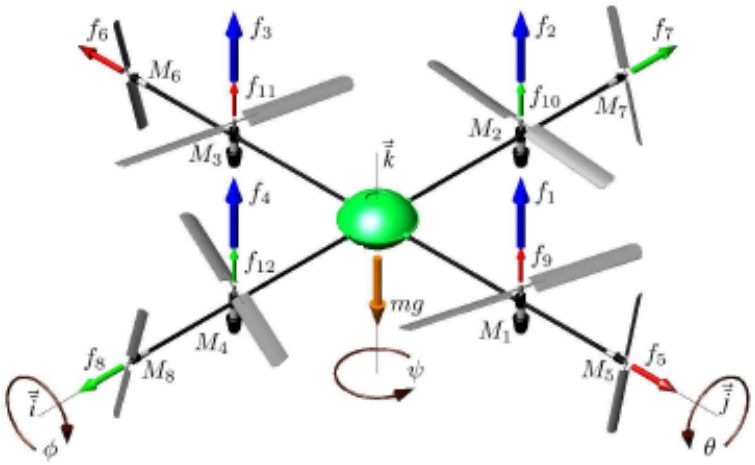

Figure 1.5: Configuration of the eight-rotor rotorcraft

1.2 Thesis structure

In this thesis, we study the attitude and position control problem for the overactuated quad-tiltrotor which has been designed in school of Engineering Design, Production Engineering and Automotive Engineering at University of Stuttgart [23]. This quad-tiltrotor allows us to independently control the position and orientation of the quad-tiltrotor at the same time. It is equipped with four extra motors, with respect to quad-rotors, to tilt the propellers. Indeed, the additional set of four control inputs actuating the propeller tilting angles is used to yield full actuation to the quad-rotor position/orientation in space, thus allowing it to behave as a fully actuated flying vehicle. A prototype of a quad-tiltrotor based on this configuration has been recently integrated at the Politecnico, see the Master thesis [18]. With respect to the control laws currently flown on the prototype, which are based on a fixed model of operation (rotor rpms to control attitude and vertical position, rotor tilt angles to control longitudinal and lateral position), in this thesis a different approach to the control law design is adopted, which allows to select the desired mode of operation dynamically. This thesis is composed of two parts.

The first part is dedicated to the mathematical modeling of the system. In this part, by exploiting Newton-Euler formulation a comprehensive and accurate mathematical model is developed. Then, some simplifications are introduced to

reduce the complicated model to a model more suited to control design. Moreover, in order to design a high performance controller and consequently obtain a satisfactory performance level, model of actuators are taken into account. In addition, an adjustable parameter β ($0 \leqslant \beta \leqslant 1$) is introduced which enables us to choose a desired mode of operation between conventional quad-rotor ($\beta = 0$) and full quad-tiltrotor ($\beta = 1$).

In the second part, we focus on control design. In this part, two optimal controllers (LQ and H_∞) are developed to control the position and attitude of the quad-tiltrotor in a desired state. These controllers are designed not only to stabilize the system, but also to ensure that the outputs track the reference inputs in presence of any disturbances. Finally, the results of several simulations are reported to illustrate the capabilities of the designed controllers.

Chapter 2

System modelling

The quad-tiltrotor is a complex mechanical system; it collects numerous physical effects from the aerodynamics and the mechanics domains. In this chapter, by using Newton-Euler formalism, a comprehensive and accurate mathematical model of the quad-tiltrotor will be derived. Since the obtained model is complex and highly nonlinear while we are dealing with a linear controller design problem, we will linearize it around an operating point. Moreover, in order to design a more accurate controller, which will be done in Chapter 3, two groups of actuators are modelled.

2.1 Preliminary definitions

Modelling starts with defining the reference frames. There are three reference frames, namely "world frame", "body frame" and "propeller frame". The world frame $F_W = \{O_W, X_W, Y_W, Z_W\}$ is a right-handed orthogonal axis-system with the origin at the quad-tiltrotor's centre of mass at the beginning of the considered motion. This reference frame is fixed to the Earth.

Body frame $F_B = \{O_B, X_B, Y_B, Z_B\}$ is a right-handed orthogonal axis-system with the origin at the quad-tiltrotor's centre of gravity. The reference frame remains fixed to the quad-tiltrotor even in perturbed motion. These two frames, world frame and body frame, are shown in Figure 2.1[1], where the symbol L represents the length of all propeller arms, $\omega_i, i = 1, ..., 4$ the propeller rotation speed and $\alpha_i, i = 1, ..., 4$ the orientation of the propeller group.

Propeller frame $F_{P_i} = \{O_{P_i}, X_{P_i}, Y_{P_i}, Z_{P_i}\}$ $i = 1, 2, 3, 4$ is the frame associated with the i-th propeller group, with X_{P_i} representing the tilting actuation axis and Z_{P_i} the propeller actuated spinning (thrust T_i) axis (see Figure 2.2[1]). Moreover, ${}^{W}R_B$ is defined as the rotation matrix representing the orientation of the body frame with respect to the world frame, while ${}^{B}R_{P_i}$ as the orientation of the propeller group i-th frame with respect to the body frame. Also $\alpha_i \in \mathbb{R}$ is the

[1]This image has been taken from [23]

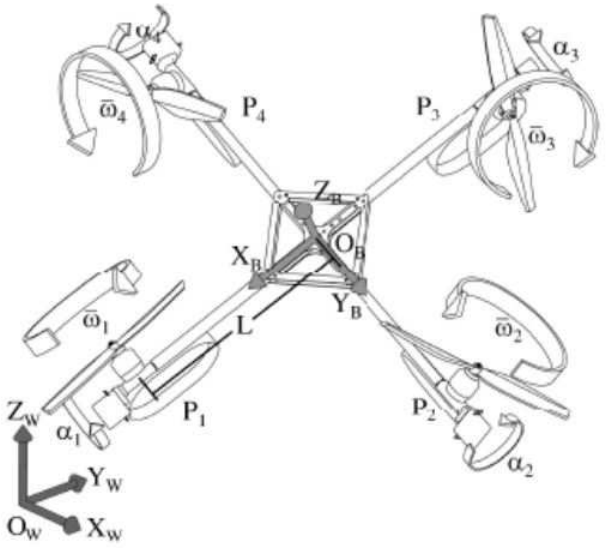

Figure 2.1: Schematic view of the quad-tiltrotor considered in this thesis.

propeller tilt angle about axis X_{P_i} as shown in Figure 2.1. Here, ${}^{B}R_{P_i}$ and ${}^{W}R_{B}$ follow as:

$$ {}^{W}R_{B} = R_Z(\psi)R_Y(\theta)R_X(\phi) = \begin{bmatrix} c_\psi c_\theta & -s_\psi c_\phi + c_\psi s_\theta s_\phi & s_\psi s_\phi + c_\psi s_\theta c_\phi \\ s_\psi c_\theta & c_\psi c_\phi + s_\psi s_\theta s_\phi & -c_\psi s_\phi + s_\psi s_\theta c_\phi \\ -s_\theta & c_\theta s_\phi & c_\theta c_\phi \end{bmatrix} \tag{2.1} $$

$$ {}^{B}R_{P_i} = R_Z((i-1)\frac{\pi}{2})R_X(\alpha_i) i = 1, \ldots, 4 \tag{2.2} $$

where $R_Z(\beta), R_Y(\beta), R_X(\beta)$ are the rotation matrices about the X, Y, Z axes of angle β, respectively and defined as follows:

$$ R_Z(\beta) = \begin{bmatrix} c_\beta & -s_\beta & 0 \\ s_\beta & c_\beta & 0 \\ 0 & 0 & 1 \end{bmatrix} \tag{2.3} $$

$$ R_Y(\beta) = \begin{bmatrix} c_\beta & 0 & s_\beta \\ 0 & 1 & 0 \\ -s_\beta & 0 & c_\beta \end{bmatrix} \tag{2.4} $$

$$ R_X(\beta) = \begin{bmatrix} 1 & 0 & 0 \\ 0 & c_\beta & -s_\beta \\ 0 & s_\beta & c_\beta \end{bmatrix} \tag{2.5} $$

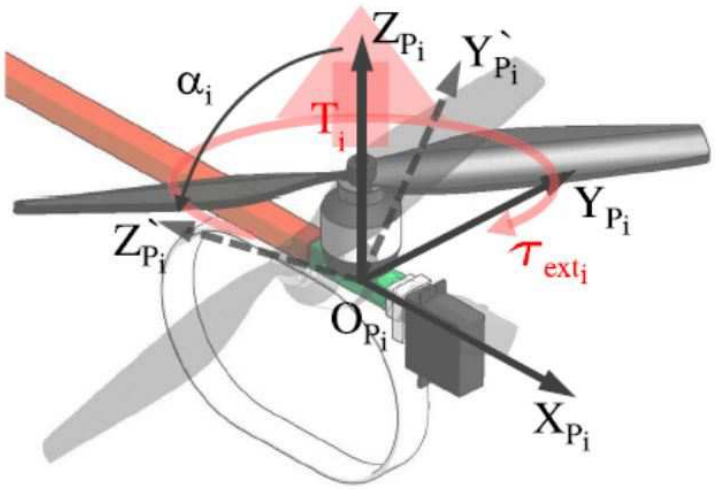

Figure 2.2: i-th tilting arm representing the body frame F_{P_i}, the associated propeller thrust T_i, torque τ_{ext_i} and the propeller tilt angle α_i.

In the previous equations this notation has been adopted: $s_k = \sin(k)$ and $c_k = \cos(k)$. Similarly we have:

$$^{B}O_{P_i} = R_Z((i-1)\frac{\pi}{2}) \begin{bmatrix} L \\ 0 \\ 0 \end{bmatrix} i = 1, \ldots, 4 \tag{2.6}$$

as the origin of the propeller frames F_{P_i} in the body frame with L being the distance of O_{P_i} from O_B. To sum up, the quad-tiltrotor configuration is determined by its position $p = {}^{W}O_B$ and orientation ${}^{W}R_B$ in world frame and four tilt angles α_i specifying the orientation of propeller groups in the body frame.

2.2 Newton-Euler equation

What one wants to obtain when deriving a model are equations of motion that describe the dynamics of the system. Within mechanics there are two common formalisms used to describe the dynamics of a plant. One is the Euler-Lagrange formalism that uses work and energy to describe the systems behaviour. The other one is the Newton-Euler formalism that uses force and torque to describe the dynamics of the system [19].

Thanks to Newton-Euler formalism, it is possible to derive an accurate dynamic model of the quad-tiltrotor, where we assumed it is a rigid body, by considering the forces/moments generated by the propeller motion as well as any

cross-coupling due to gyroscopic and inertial effects arising from the relative motion of the components composing the quad-tiltrotor. Newton-Euler equation consists of translational motion, Newton's law, and rotational motion, Euler's law. Newton's law is as follows:

$$m\dot{v}_B + \omega_B \times mv_B = F_B \tag{2.7}$$

where $\dot{v}_B$ and F_B are body velocity and body force respectively. While Euler's law is as follows:

$$I_B\dot{\omega}_B + \omega_B \times I_B\omega_B = T_B. \tag{2.8}$$

Here I_B, ω_B and T_B are inertia tensor, body angular velocity and body moments respectively. Our objective is to obtain the rotational motion of quad-tiltrotor in the body frame and translational motion in the world frame.

2.2.1 Rotational motion

Firstly, we obtain all the moments applied to the propellers. Secondly, we compute all the moments applied to the body. Finally, we will be able to calculate the body angular acceleration. Let $\omega_B \in \mathbb{R}^3$ be the angular velocity of the quad-tiltrotor body B expressed in the body frame, and consider the i-th propeller group P_i. The angular velocity of the i-th propeller (i.e., of F_{P_i}) w.r.t. F_W and expressed in F_{P_i} is:

$$\omega_{P_i} = {}^B R_{P_i}^T \omega_B + \begin{bmatrix} \dot{\alpha}_i \\ 0 \\ \bar{\omega}_i \end{bmatrix} \tag{2.9}$$

where $\dot{\alpha}_i$ is the tilting velocity about X_{P_i} and $\bar{\omega}_i \in \mathbb{R}$ is the spinning velocity about Z_{P_i} both w.r.t. F_B . Then, angular acceleration is as follows:

$$\dot{\omega}_{P_i} = {}^B R_{P_i}^T \dot{\omega}_B + {}^B \dot{R}_{P_i}^T \omega_B + \begin{bmatrix} \ddot{\alpha}_i \\ 0 \\ \dot{\bar{\omega}}_i \end{bmatrix}. \tag{2.10}$$

Using the Euler's law, it follows as:

$$\tau_{P_i} = I_{P_i}\dot{\omega}_{P_i} + \omega_{P_i} \times I_{P_i}\omega_{P_i} - \tau_{ext_i} \tag{2.11}$$

where $I_{P_i} \in \mathbb{R}^{3\times3}$ is the constant symmetric and positive definite inertia matrix of the i-th propeller, and τ_{ext_i} any other external torques applied to the propeller. We suppose that air drag causes a counter-rotating torque about the Z_{P_i} axis and model it as has been done in [20]:

$$\tau_{ext_i} = \begin{bmatrix} 0 & 0 & -k_m\omega_{P_{i_Z}} \left|\omega_{P_{i_Z}}\right| \end{bmatrix}^T, k_m > 0 \tag{2.12}$$

with $\omega_{P_{i_Z}}$ being the third component of ω_{P_i}. Let's now introduce the i-th propeller force (thrust) along the Z_{P_i} axis and acting at origin of the propeller frames F_{P_i} in the body frame (i.e., ${}^{B}O_{P_i}$) as follows:

$$T_{p_i} = \begin{bmatrix} 0 & 0 & k_f \bar{\omega}_i \left|\bar{\omega}_i\right| \end{bmatrix}^T, k_f > 0. \tag{2.13}$$

Now, by considering the quad-tiltrotor body and the torques generated by the four propellers P_i, one can obtain

$$\sum_{i=1}^{4} ({}^{B}O_{p_i} \times {}^{B}R_{p_i} T_{p_i} - {}^{B}R_{p_i} \tau_{p_i}) = I_B \dot{\omega}_B + \omega_B \times I_B \omega \tag{2.14}$$

with $I_B \in \mathbb{R}^{3\times 3}$ being the constant symmetric and positive definite inertia matrix of body. In order to design a controller we have to transform equation (2.14) to a proper form, then it needs to be written as follows:

$$\dot{\omega}_B = \begin{bmatrix} \dot{p} \\ \dot{q} \\ \dot{r} \end{bmatrix} = \left[I_B + \sum_{i=1}^{4} {}^{B}R_{p_i} I_{P_i} {}^{B}R_{p_i}{}^{T} \right]^{-1} .$$
$$\left[\sum_{i=1}^{4} {}^{B}O_{p_i} \times {}^{B}R_{p_i} T_{p_i} - \sum_{i=1}^{4} {}^{B}R_{p_i} (I_{P_i} \begin{bmatrix} \ddot{\alpha}_i \\ 0 \\ \dot{\omega}_i \end{bmatrix} + (\omega_{P_i} \times I_{P_i} \omega_{P_i}) - \tau_{ext_i}) - \omega_B \times I_B \omega_B \right] . \tag{2.15}$$

For the reader's convenience, Table 2.1 lists the main quantities introduced in this section and Table 2.2 presents the constant value of quantities which are taken from [23].

Table 2.1: Main quantities and definitions of the quad-tiltrotor

Symbols	Definitions
F_w	inertial world frame
F_b	quad-tiltrotor body frame B
F_{P_i}	i-th propeller group frameP_i
p	position of B in F_w
${}^{W}R_B$	rotation matrix from F_B to F_w
${}^{B}R_{P_i}$	rotation matrix from F_{P_i} to F_B
α_i	i-th propeller tilt angle about X_{P_i}
$\bar{\omega}_i$	i-th propeller spinning velocity about Z_{P_i}
ω_B	angular velocity of B in F_B
τ_{ext_i}	i-th propeller air drag torque about Z_{P_i}
T_i	i-th propeller thrust along Z_{P_i}
τ_{P_i}	motor torque actuating X_{P_i}
m	total mass
I_P	inertia of the i-th propeller group P_i
I_B	inertia of the quad-tiltrotor body$B$
k_f	propeller thrust coefficient
k_m	propeller drag coefficient
L	distance of F_{P_i} from F_B
g	gravitational acceleration of Earth

Table 2.2: Values of parameters of the quad-tiltrotor model

Symbols	Values	units
m	1.32	kg
g	9.81	m/s^2
L	0.5	m
k_m	2.5278×10^{-7}	–
K_f	1.5601×10^{-5}	–
I_B	$\begin{bmatrix} 0.0154 & 0 & 0 \\ 0 & 0.0154 & 0 \\ 0 & 0 & 0.0263 \end{bmatrix}$	$kg.m^2$
I_P	$\begin{bmatrix} 8.45 \times 10^{-5} & 0 & 0 \\ 0 & 8.45 \times 10^{-5} & 0 \\ 0 & 0 & 4.58 \times 10^{-5} \end{bmatrix}$	$kg.m^2$

2.2.2 Translational motion

To simplify the translational dynamics, it is assumed that the center of mass of each propeller group P_i coincides with O_{P_i}. In this way we can ignore inertial effects on the propeller groups arising from quad-tiltrotor body acceleration in space. As usual it is more convenient to express the position of quad-tiltrotor in world frame because variation of position makes more sense in this frame. Therefore, by recalling that $p = {}^{W}O_B$ is the quad-tiltrotor body position in world frame and using equation (2.7) one obtains

$$m\ddot{p} = m \begin{bmatrix} 0 \\ 0 \\ -g \end{bmatrix} + {}^{W}R_B \sum_{i=1}^{4} {}^{B}R_{p_i} T_{p_i} \tag{2.16}$$

where m is the total mass of the quad-tiltrotor and propeller bodies and the scalar gravitational acceleration of Earth.

To sum up, equations (2.15) and (2.16) describe the full model of the quad-tiltrotor. Now we can use this full and precise model of quad-tiltrotor for designing our controller.

2.3 Simplified quad-tiltrotor model

Although the dynamic model obtained in the previous section is useful for simulation purposes as it captures the main effects of quad-tiltrotor motion in space (except unmodeled aerodynamic forces and torques which are considered as external disturbances to be rejected by the controller), some simplifications are however useful for transforming it to a model more suited to control design. To simplify the full dynamic model, we neglect the internal gyroscopic/inertial effects by considering them as second-order disturbances to be rejected by the controller. Since the inertia matrix of propellers is negligible in comparison with the inertia matrix of the body we can also ignore its effect on the dynamic model. Therefore the simplified model can be written as follows:

$$\dot{\omega}_B = \begin{bmatrix} \dot{p} \\ \dot{q} \\ \dot{r} \end{bmatrix} = {I_B}^{-1} \left[\sum_{i=1}^{4} {}^{B}O_{p_i} \times {}^{B}R_{p_i} T_{p_i} + \sum_{i=1}^{4} {}^{B}R_{p_i} \tau_{ext_i} \right] \tag{2.17}$$

$$\ddot{p} = \begin{bmatrix} \dot{X} \\ \dot{Y} \\ \dot{Z} \end{bmatrix} = \begin{bmatrix} 0 \\ 0 \\ -g \end{bmatrix} + \frac{1}{m} {}^{W}R_B \sum_{i=1}^{4} {}^{B}R_{p_i} T_{p_i} \tag{2.18}$$

2.4 Calculation of hovering state

In flying near hovering with level attitude, the tilting angles $\alpha_1, \ldots, \alpha_4$ are assumed to be zero and the quad-tiltrotor becomes a conventional quadrotor. Now for a conventional quadrotor the equations that govern the hovering motion are the equations of equilibrium as well as the equations of power:

$$\begin{array}{l} \sum F_x = 0 \Rightarrow 0 = 0 \\ \sum F_y = 0 \Rightarrow 0 = 0 \\ \sum F_z = 0 \Rightarrow \mathrm{T}_1{+}\mathrm{T}_2 + \mathrm{T}_3 + \mathrm{T}_4{=}mg \\ \sum M_x = 0 \Rightarrow \mathrm{T}_2L{=}\mathrm{T}_4L \\ \sum M_y = 0 \Rightarrow \mathrm{T}_1L{=}\mathrm{T}_3L \\ \sum M_z = 0 \Rightarrow \mathrm{Q}_1{-}\mathrm{Q}_2{+}\mathrm{Q}_3{-}\mathrm{Q}_4{=}\,0 \\ \mathrm{Q}_i = R_eT_i \end{array} \tag{2.19}$$

Recall that T_i is the thrust force corresponding to ω_i, m is the mass of quad-tiltrotor, g is the gravity acceleration, L is the distance between two rotors of the same axis, Q_i is the moment created by the rotor i, and finally $R_e = r_r\frac{C_P}{C_T}$ being r_r the radius of the rotor, C_p the coefficient of power and C_r the coefficient of thrust.

This system has 4 unknown quantities and 3 linearly independent equations, so it has infinite solutions. One possible solution is:

$$T_1 = T_2 = T_3 = T_4 = \bar{T} \tag{2.20}$$

Where $\bar{T} = \frac{mg}{4}$. By recalling that $T_i = k_f\bar{\omega}_i\left|\bar{\omega}_i\right|$, the rotor spinning velocity at hovering state is equal to $455.53\,[rad/s]$.

2.5 Linearized quad-tiltrotor model

Since we are dealing with a linear controller design problem, we must linearize the nonlinear dynamical model around an operating point. Most physical systems are nonlinear [21]. Some of them can be described by the state space model

$$\begin{array}{l} \dot{x}(t) = f(x(t), u(t)) \\ y(t) = g(x(t), u(t)) \end{array} \tag{2.21}$$

where f and g are nonlinear functions. Some nonlinear equations, however, can be approximated by linear equations under certain conditions. Assuming a constant input $u_0(t)$ and initial state $x_0(t)$, the solution of equation (2.21) is

$$\dot{x}_0(t) = f(x_0(t), u_0(t)) = 0. \tag{2.22}$$

Now suppose the input is perturbed slightly to become $u_0(t)+\bar{u}(t)$ and the initial state is also perturbed only slightly. For some nonlinear equations, the corresponding solution may differ from $x_0(t)$ only slightly. In this case, the solution

can be expressed as $x_0(t) + \bar{x}(t)$ with $\bar{x}(t)$ small for all t. Under this assumption and using a Taylor series expansion for $\dot{x}(t) = f(x(t), u(t))$ we can write

$$\dot{x}(t)=f(x_0(t), u_0(t)) + \left.\frac{\partial f}{\partial x}\right|_{x_0,u_0} (x - x_0) + \left.\frac{\partial f}{\partial u}\right|_{x_0,u_0} (u - u_0) + \text{higher order terms.} \tag{2.23}$$

According to equation (2.22) and neglecting the higher order terms, equation (2.23) can be written as

$$\dot{x}(t) \approx \left.\frac{\partial f}{\partial x}\right|_{x_0,u_0} (x - x_0) + \left.\frac{\partial f}{\partial u}\right|_{x_0,u_0} (u - u_0) \tag{2.24}$$

Since the derivative of a constant value is zero we can write

$$\dot{x}(t) = \dot{x}(t) - \dot{x}_0(t) = \dot{\bar{x}}(t) \tag{2.25}$$

Finally, the state-space form of a linearized system is as follows:

$$\dot{\bar{x}}(t) = A\bar{x}(t) + B\bar{u}(t) \tag{2.26}$$

where

$$\begin{aligned} A &:= \left.\tfrac{\partial f}{\partial x}\right|_{x_0,u_0} := \begin{pmatrix} \left.\frac{\partial f_1}{\partial x_1}\right|_{x_0,u_0} & \cdots & \left.\frac{\partial f_1}{\partial x_n}\right|_{x_0,u_0} \\ \vdots & \ddots & \vdots \\ \left.\frac{\partial f_n}{\partial x_1}\right|_{x_0,u_0} & \cdots & \left.\frac{\partial f_n}{\partial x_1}\right|_{x_0,u_0} \end{pmatrix} \\ B &:= \left.\tfrac{\partial f}{\partial u}\right|_{x_0,u_0} := \begin{pmatrix} \left.\frac{\partial f_1}{\partial u_1}\right|_{x_0,u_0} & \cdots & \left.\frac{\partial f_1}{\partial u_n}\right|_{x_0,u_0} \\ \vdots & \ddots & \vdots \\ \left.\frac{\partial f_n}{\partial u_1}\right|_{x_0,u_0} & \cdots & \left.\frac{\partial f_n}{\partial u_1}\right|_{x_0,u_0} \end{pmatrix} \end{aligned} \tag{2.27}$$

This is a linear state-space equation. The equation $y(t) = g(x(t), u(t))$ can be similarly linearized. Now to proceed the linearization, we should transform equations (2.17) and 2.18 to the state-space form, then using formula (2.27) a linear state-space form will be obtained. The transformation matrix between the rate of change of orientation angles $(\ \dot{\phi} \quad \dot{\theta} \quad \dot{\psi}\ )$ and body angular velocities $(\ p \quad q \quad r\ )$ can be considered as unity matrix since we are working around hovering state and perturbations are assumed to be small. Then, one can write $(\ \dot{\phi} \quad \dot{\theta} \quad \dot{\psi}\ ) \approx (\ p \quad q \quad r\ )$.
The state vector is chosen as follows:

$$x = \left[\ X\ \dot{X}\ Y\ \dot{Y}\ Z\ \dot{Z}\ \phi\ \dot{\phi}\ \theta\ \dot{\theta}\ \psi\ \dot{\psi}\ \right]^T \tag{2.28}$$

while the input vector defined as:

$$u = \begin{bmatrix} \bar{\omega}_1 & \bar{\omega}_2 & \bar{\omega}_3 & \bar{\omega}_4 & \alpha_1 & \alpha_2 & \alpha_3 & \alpha_4 \end{bmatrix}^T \tag{2.29}$$

and the output is given by the quad-tiltrotor's position and orientation; it means that the output vector is as below:

$$y = \begin{bmatrix} X & Y & Z & \phi & \theta & \psi \end{bmatrix}^T. \tag{2.30}$$

Eventually, the operating point where linearization is done is as follows:

$$\begin{aligned} x_0 &= \begin{bmatrix} 0 & 0 & 0 & 0 & 0 & 0 & 0 & 0 & 0 & 0 & 0 & 0 \end{bmatrix}^T \\ u_0 &= \begin{bmatrix} 455.53 & -455.53 & 455.53 & -455.53 & 0 & 0 & 0 & 0 \end{bmatrix}^T \end{aligned} \tag{2.31}$$

By exploiting equations (2.17) and (2.18) around the hovering state, matrices A, B, C and then the full state-space model can be obtained (see appendix A).

2.6 Model of actuators

There are eight DC-motors acting as actuators: four of them are responsible for producing the spinning velocity of the propellers and the others are in charge of tilting the propellers. Therefore, totally we have eight DC-motors used in this quad-tiltrotor. Electric DC motors are well modeled by a circuit containing a resistor, inductor, and voltage generator in series. Equivalent motor circuit can be represented as Figure 2.3 where e is the counter electromotive force, v is the applied voltage, i is the current, θ is the angular rotation of the rotor relative to the stator, R is the electric resistance, L is the electric inductance and b is the motor viscous friction constant.

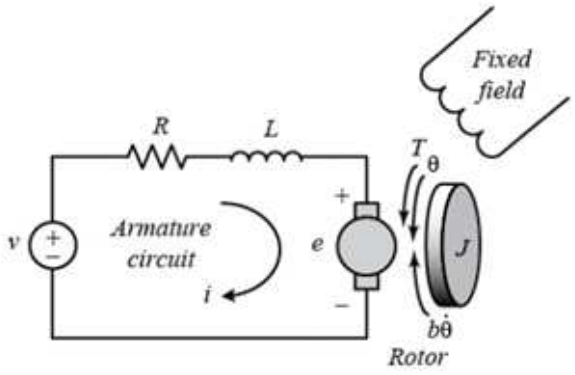

Figure 2.3: Electrical and mechanical schematic of equivalent motor circuit

Kirchhoff's law applied to the equivalent motor circuit yields

$$v = Ri + L\frac{di}{dt} + k_e\omega \tag{2.32}$$

while mechanical load is

$$J\ddot{\theta} + b\dot{\theta} = k_t i \tag{2.33}$$

where k_e is the electromotive force constant and k_t is the motor torque constant. Now the transfer function from voltage as input to angular velocity as output is as follows

$$\frac{\omega(s)}{v(s)} = \frac{k_t}{(Js+b)(Ls+R) + k_t k_e}. \tag{2.34}$$

In many cases $L << R$. Then, an approximate transfer function can be obtained by setting $L = 0$. Therefore, the transfer function reduces from second order system to a first order system.

$$\frac{\omega(s)}{v(s)} \approx \frac{k_t}{R(Js+b) + k_t k_e} =: \frac{K}{Ts+1}. \tag{2.35}$$

In this thesis, gain k and time constant T are derived from [22]. Then, the model of the main motors, i.e., responsible for producing spinning velocities, becomes

$$T_\omega = \frac{1}{0.125s+1} \tag{2.36}$$

moreover, we assume that the motors responsible for tilting the propellers are slower than the main motors by 50%.

$$T_\alpha = \frac{1}{0.25s+1}. \tag{2.37}$$

Chapter 3

Control design

In this chapter we are going to design optimal controllers to control the attitude and the position of the quad-tiltrotor in the presence of disturbances. Since this quad-tiltrotor is an overactuated system with 6 outputs and 8 inputs, we are able to control both its position and attitude simultaneously. First, a linear quadratic (LQ) optimal controller is designed. Second, an optimal H_∞ controller will be developed. Then, the results obtained by these two controllers are compared. Finally, the performance of LQ and H_∞ controllers in presence of model uncertainty will be verified.

3.1 Modelling for control

The linearized model obtained in Subsection 2.5 still is not ready for designing a controller, because model of actuators which were introduced in the system in Subsection 2.6 can affect the overall performance of the system. Therefore, in order to design a high performance controller and consequently obtain a satisfactory performance level, actuators dynamics must be taken into account. Hence, to obtain the final model, actuators dynamics should be added to the linearized model by introducing them as new states. Recalling that the model of the main motors, i.e., responsible for producing spinning velocities, is

$$T_\omega = \frac{y_\omega}{u_\omega} = \frac{1}{0.125s + 1} \tag{3.1}$$

that it can be written as

$$\dot{y}_\omega = -8y_\omega + 8u_\omega \ . \tag{3.2}$$

Also, the model of the motors responsible for tilting the propellers, is

$$T_\alpha = \frac{y_\alpha}{u_\alpha} = \frac{1}{0.25s + 1} \tag{3.3}$$

that can be shown as

$$\dot{y}_\alpha = -4y_\alpha + 4u_\alpha \ . \tag{3.4}$$

Finally, the state-space form of the final model to be controlled is as follows:

$$\begin{aligned} \dot{x}(t) &= A_a x(t) + B_a u(t) \\ y(t) &= C_a x(t) \end{aligned} \tag{3.5}$$

where new states and input vectors are as below

$$x = \left[\ X \ \dot{X} \ Y \ \dot{Y} \ Z \ \dot{Z} \ \phi \ \dot{\phi} \ \theta \ \dot{\theta} \ \psi \ \dot{\psi} \ \ y_{\omega_1} \ y_{\omega_2} \ y_{\omega_3} \ y_{\omega_4} \ y_{\alpha_1} \ y_{\alpha_2} \ y_{\alpha_3} \ y_{\alpha_4} \ \right]^T \tag{3.6}$$

$$u = \left[\ u_{\omega_1} \ u_{\omega_2} \ u_{\omega_3} \ u_{\omega_4} \ u_{\alpha_1} \ u_{\alpha_2} \ u_{\alpha_3} \ u_{\alpha 4} \ \right]^T. \tag{3.7}$$

New matrices A_a, B_a and C_a in (3.5) can be found in Appendix A.

3.2 Reference tracking

In SISO and MIMO systems, it is possible to guarantee a null steady state error by forcing an integral action on each component of the error signal, as shown in Figure 3.1, where $R(s)$ and $G(s)$ are the regulator and the system, respectively. For constant set-point or disturbances on the output, all the signals in the loop tend to a constant value. Observe also that the integral action guarantees robust zero error regulation, i.e., also for small process parameter perturbations or model errors, provided that the closed-loop stability is maintained [24].

3.2.1 Conditions of reference tracking design

Assume the system under control is

$$\begin{aligned} \dot{x}(t) &= Ax(t) + Bu(t) + Md \\ y(t) &= Cx(t) + Nd \end{aligned} \tag{3.8}$$

where $x \in \mathbb{R}^n$, $u \in \mathbb{R}^m$, $y \in \mathbb{R}^p$, and $d \in \mathbb{R}^r$ is a constant disturbance acting on the state and on the output. For this system, it is required that, at the steady state, $y = y^0$ for any constant y^0 and d.

Denoting with barred symbols the steady state variables, to guarantee zero steady state error the following relations must hold

$$\begin{aligned} 0 &= A\bar{x} + B\bar{u} + Md \\ y^0 &= C\bar{x} + Nd \qquad . \end{aligned} \tag{3.9}$$

Relation (3.9) can be written as

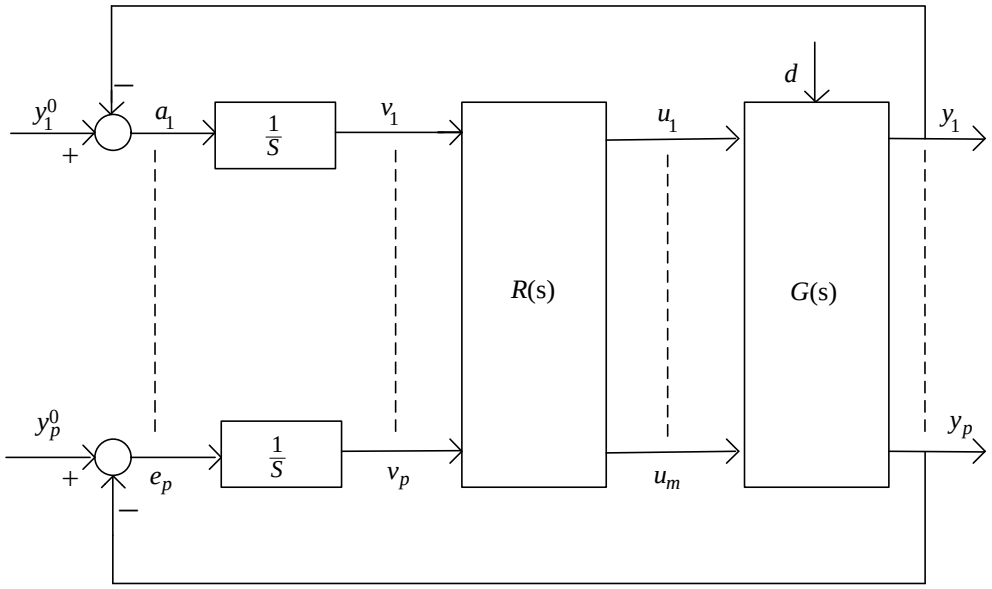

Figure 3.1: Scheme with integral action on the error for MIMO systems

$$\begin{bmatrix} A & B \\ C & 0 \end{bmatrix} \begin{bmatrix} \bar{x} \\ \bar{u} \end{bmatrix} = \begin{bmatrix} 0 & -M \\ I & -N \end{bmatrix} \begin{bmatrix} y^0 \\ d \end{bmatrix}. \tag{3.10}$$

Now note that

$$\sum = \begin{bmatrix} A & B \\ C & 0 \end{bmatrix} \in \mathbb{R}^{n+p,n+m}. \tag{3.11}$$

Therefore, the conditions

1. $p \leqslant m$
2. $rank(\sum) = n + p$

must hold to guarantee that there exist at least a pair $\bar{x}$, $\bar{u}$ satisfying the relation (3.10) for any constant y^0 and d [24].

In relation (3.5), $p = 6$ and $m = 8$, then the first condition holds.

Moreover,

$$rank(\sum = \begin{bmatrix} A_a & B_a \\ C_a & 0 \end{bmatrix}) = m + p = 26.$$

Since both conditions are satisfied, we can guarantee that there exist at least a pair $\bar{x},\ \bar{u}$ satisfying the relation (3.10) for any constant y^0 and d.

3.2.2 Enlarged system

By considering Figure 3.1, the integrators in state variables are described by

$$\begin{aligned} \dot{v}(t) &= e(t) \\ &= y^0 - y(t) \\ &= y^0 - Cx(t) - Nd \end{aligned} \tag{3.12}$$

Hence, the enlarged system made by the process and the integrators, with manipulable input u and measured output y is

$$\begin{aligned} \begin{bmatrix} \dot{x}(t) \\ \dot{v}(t) \end{bmatrix} &= \begin{bmatrix} A_a & 0 \\ -C_a & 0 \end{bmatrix} \begin{bmatrix} x(t) \\ v(t) \end{bmatrix} + \begin{bmatrix} B_a \\ 0 \end{bmatrix} u(t) + \begin{bmatrix} 0 & M \\ I & -N \end{bmatrix} \begin{bmatrix} y^0 \\ d \end{bmatrix} \\ y(t) &= \begin{bmatrix} C_a & 0 \end{bmatrix} \end{aligned} \tag{3.13}$$

Defining

$$\bar{A} = \begin{bmatrix} A_a & 0 \\ -C_a & 0 \end{bmatrix}, \bar{B} = \begin{bmatrix} B_a \\ 0 \end{bmatrix}, \bar{\mathrm{C}} = \begin{bmatrix} C_a & 0 \end{bmatrix}. \tag{3.14}$$

3.3 Linear quadratic optimal control

State feedback controllers using pole placement algorithms are one of the basic and fundamental controllers for linear systems. These controllers are developed based on the desired closed loop poles. For single input systems, given a set of desired eigenvalues, the feedback gain to achieve this is unique (as long as the system is controllable). For multi-input systems, the feedback gain is not unique, so there is additional design freedom. A more fundamental issue is that the choice of eigenvalues is not obvious. For example, there are trade offs between robustness, performance, and control effort.

Linear quadratic (LQ) optimal control can be used to resolve some of these issues, by not specifying exactly where the closed loop eigenvalues should be directly, but instead by specifying some kind of performance objective function to be optimized [25].

Consider the following linear time invariant system, with initial time $t_0 = 0$ and measurable state

$$\dot{x}(t) = Ax(t) + Bu(t), \quad x(0) = x_0 \tag{3.15}$$

and the performance index

$$J(x_0, u(\cdot), 0) = \int_0^\infty (x^T(\tau)Qx(\tau) + u^T(\tau)Ru(\tau))d\tau \tag{3.16}$$

which can be written as

$$J(x_0, u(\cdot), 0) = \int_0^\infty \begin{bmatrix} x(\tau) \\ u(\tau) \end{bmatrix}^T \begin{bmatrix} Q & 0 \\ 0 & R \end{bmatrix} \begin{bmatrix} x(\tau) \\ u(\tau) \end{bmatrix} d\tau \tag{3.17}$$

where

$$Q = Q^T \geqslant 0, \ R = R^T > 0$$

are design parameters. The aim of LQ optimal control is to minimizing the cost function presented in (3.17). To minimize this function, one should solve Riccati equation which is defined as bellow

$$\dot{P}(t) + Q - P(t)BR^{-1}B^TP^T(t) + A^TP^T(t) + P(t)A = 0 \tag{3.18}$$

and the corresponding control law is

$$u(t) = -R^{-1}B^TP^T(t)x(t) = -K(t)x(t). \tag{3.19}$$

Theorem 3.3.1. If the pair (A, B) is reachable:

1. The soloution of the differential Riccati equation with initial condition $P(T) = 0$ tends, for $T \to \infty$, to a constant matrix $\bar{P} \geqslant 0$ solution of the algebraic Riccati equation

$$0 = A^T\bar{P} + \bar{P}A + Q - \bar{P}BR^{-1}B^T\bar{P}$$

2. The asymptotic control law is

$$u(t) = -R^{-1}B^T\bar{P}x(t) = -\bar{K}x(t) \tag{3.20}$$

where $\bar{K} = R^{-1}B^T\bar{P}$.

Matrix $\bar{P}$ solves the Riccati equation, and in view of the continuity of this equation and the assumption $Q \geqslant 0, \ R > 0$, it is symmetric and positive semidefinite [24]. Therefore, the closed loop system follows as

$$\dot{x}(t) = Ax(t) - B\bar{K}x(t) = (A - BR^{-1}B^T\bar{P})x(t). \tag{3.21}$$

Now we are going to design a LQ controller for the enlarged system (3.14) by choosing proper matrices Q and R.

The purpose of this thesis is to control the quad-tiltrotor in a desired mode of operation. We define the operation mode as the size of cooperation between the primary motors and the secondary motors. For example, when the operation mode is equal to 0.5, the lateral movement caused by 50% primary motors and 50% secondary motors and when it is equal to 0.2, the lateral movement is done by 20% primary motors and 80% secondary motors and so on. As a result, the operation mode is a number between 0 and 1 (it is zero when the system is working as a conventional quad-rotor and is equal to one when the system is working as a full quad-tiltrotor).

To make this definition implementable for control design, an adjustable parameter β ($0 \leqslant \beta \leqslant 1$) is introduced which enables us to choose our desired mode of operation. In order to achieve our goal, we need to set a linear relation between β and the operation mode in practice, such as the blue line in Figure 3.2.

The basic idea to construct Q and R matrices is

$$Q = (1-\beta)Q_\omega + \beta Q_\alpha$$
$$R = (1-\beta)R_\omega + \beta R_\alpha.$$

where index ω represents that only primary motors, those are responsible for producing spinning velocities, work as actuators and secondary motors which are responsible for tilting the propellers are deactivated (the tilting angles are set to zero). Index α represents that all four primary motors have the same spinning velocity (they are only responsible for hovering state and altitude movement), while secondary motors are in charge of lateral movements.

Here, Q_ω and R_ω are designed for a conventional quad-rotor independent of full quad-tiltrotor. Also Q_α and R_α are chosen for a full quad-tiltrotor independent of conventional quad-rotor. Finally, both of them are combined through the parameter β.

Hence, by putting $\beta = 0$ the system becomes a conventional quad-rotor and by setting $\beta = 1$ we can have a full quad-tiltrotor which is able to move laterally without tilting the body.

But the linear combination of Q_ω and Q_α (R_ω and R_α) results in a nonlinear relation between β and the operation mode of the quad-tiltrotor (yellow curve in Figure 3.2). Thus, we have increased the power of β as long as the ideal behavior is reached (red curve in Figure 3.2). Therefore, four experiments have been carried out in which the operation mode is measured[1] for some specific value

[1] Operation mode$=\frac{\alpha_j(\beta)}{\alpha_j(\beta=1)}$ j :working secondary motor

of β for the following design parameters:

Experiment 1:

$$Q = (1-\beta)Q_\omega + \beta Q_\alpha$$
$$R = (1-\beta)R_\omega + \beta R_\alpha$$

Experiment 2:

$$Q = (1-\beta^2)Q_\omega + \beta^2 Q_\alpha$$
$$R = (1-\beta^2)R_\omega + \beta^2 R_\alpha$$

Experiment 3:

$$Q = (1-\beta^3)Q_\omega + \beta^3 Q_\alpha$$
$$R = (1-\beta^3)R_\omega + \beta^3 R_\alpha$$

Experiment 4:

$$Q = (1-\beta^4)Q_\omega + \beta^4 Q_\alpha$$
$$R = (1-\beta^4)R_\omega + \beta^4 R_\alpha.$$

Table 3.1 shows the data collected from the four aforementioned experiments. The set of data (β, operation mode) for each experiment is used to plot a continuous curve by means of linear interpolation method.

Table 3.1: Operation mode of four experiments for different value of β

β	operation mode in experiment 1	operation mode in experiment 2	operation mode in experiment 3	operation mode in experiment 4
0	0	0	0	0
0.2	0.71	0.41	0.18	0.1
0.4	0.813	0.66	0.5	0.33
0.5	0.83	0.750	0.63	0.5
0.6	0.85	0.8	0.73	0.64
0.8	0.9	0.83	0.83	0.816
1	1	1	1	1

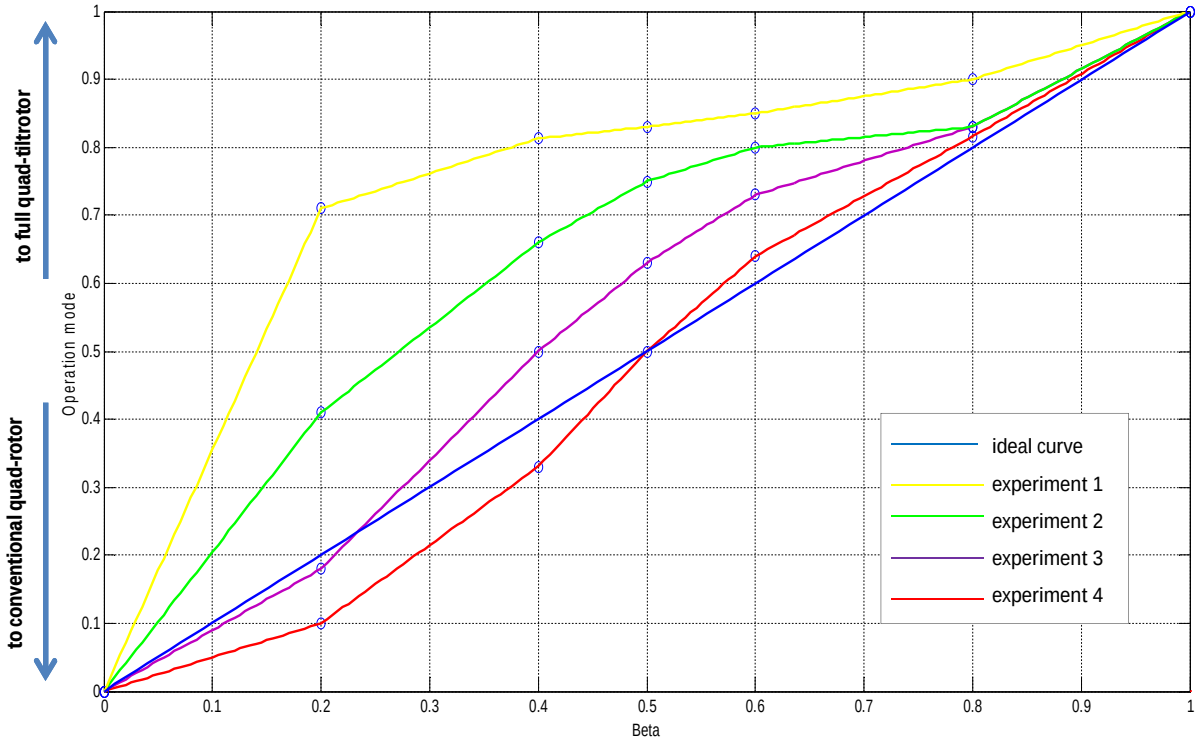

Figure 3.2: β versus the operation mode of the quad-tiltrotor for different experiments

Figure 3.2 shows that the experiment 4 is close to the ideal curve. As a result, design parameters Q and R used in these thesis are constructed as done in experiment 4.

Now, we are going to design a position and attitude controller for the enlarged system described in Section 3.2.2. Considering Theorem 3.3.1, since pair $(\bar{A}, \bar{B})$ is reachable, it is possible to design a controller to achieve our goals. The block diagram of the associated control system is shown in Figure 3.3, where $G(s)$ is the system presented in equation (3.5), LQ represents the controller designed by LQ technique and input β is the operation mode adjustment of the quad-tiltrotor.

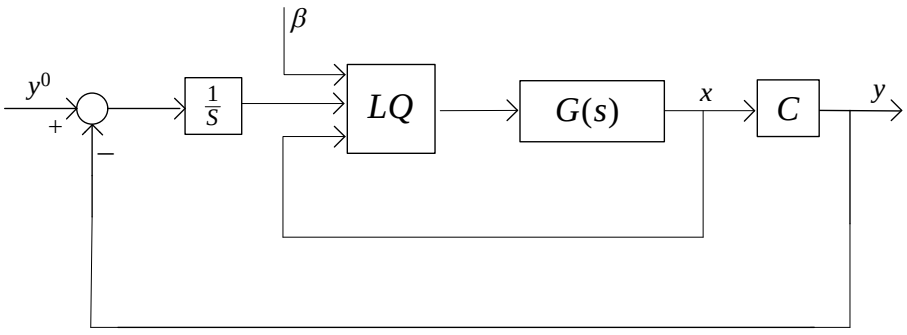

Figure 3.3: Block diagram of the LQ control algorithm

The block diagram of the control system shown in Figure 3.3 is implemented in *Simulink* and required parameters are taken from $MATLAB$ workspace. The

Simulink block diagram of the system is illustrated below in Figure 3.4.

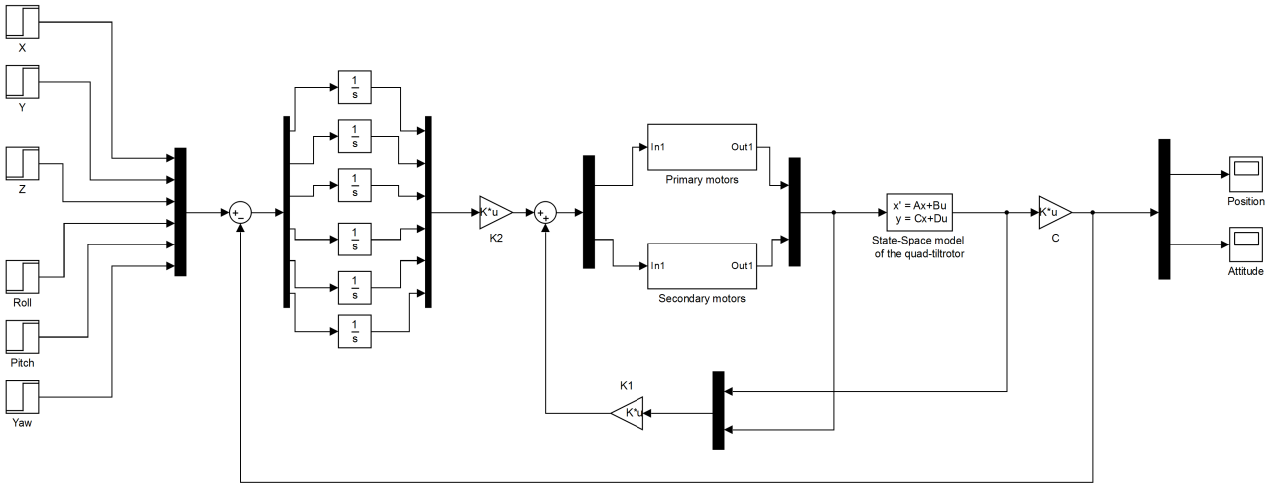

Figure 3.4: Block diagram of the LQ control algorithm implemented in *Simulink*

The gain matrix $\bar{K}$ is calculated using $MATLAB$ and is separated into K_1 corresponding to the state feedback and K_2 corresponding to the integral gain.

3.3.1 Position control

By choosing proper Q and R matrices (see appendix B) a LQ position controller is designed not only to stabilize the system, but also to ensure that the outputs track the reference inputs. By changing the parameter β, we will investigate the different operation modes of the quad-tiltrotor to see the controller performance in case of reference tracking.

Different modes of quad-tilt-rotor without external disturbances

Here, the quad-tiltrotor is assumed to be at hovering state; after two seconds it is forced to move five meters along the X_W direction while there are no disturbances. In Figures 3.5, 3.6 and 3.7 the controller performance for three modes of quad-tiltrotor ($\beta = 0,\ \beta = 0.5,\ \beta = 1$), is shown.

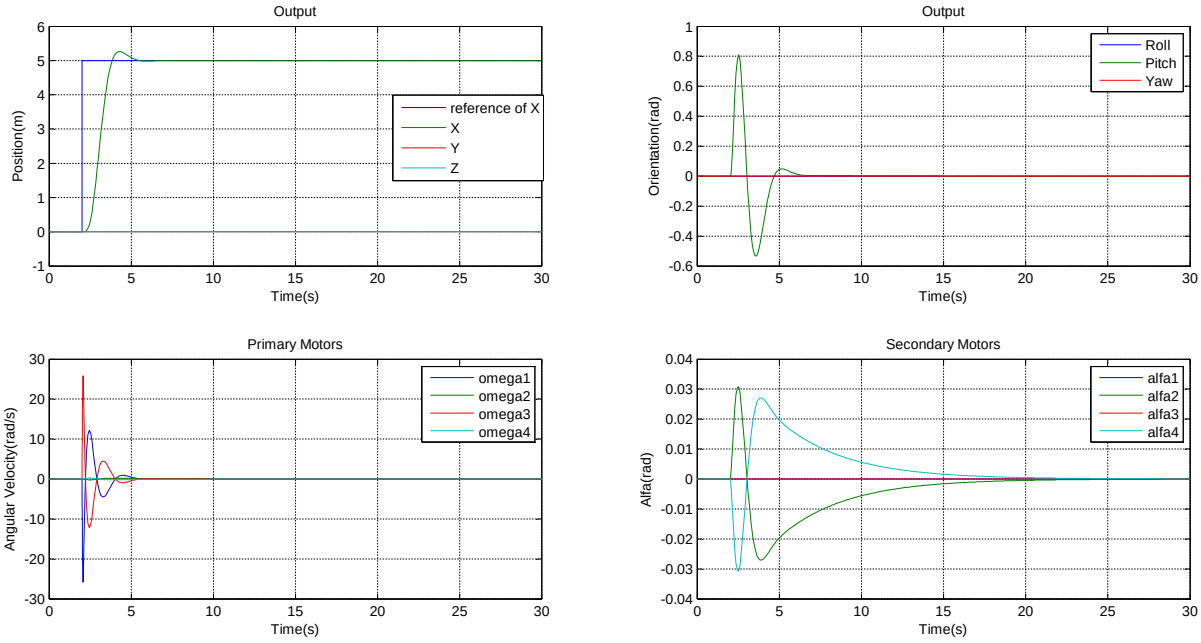

Figure 3.5: Position control of the quad-tiltrotor without any disturbances for operation mode $\beta = 0$

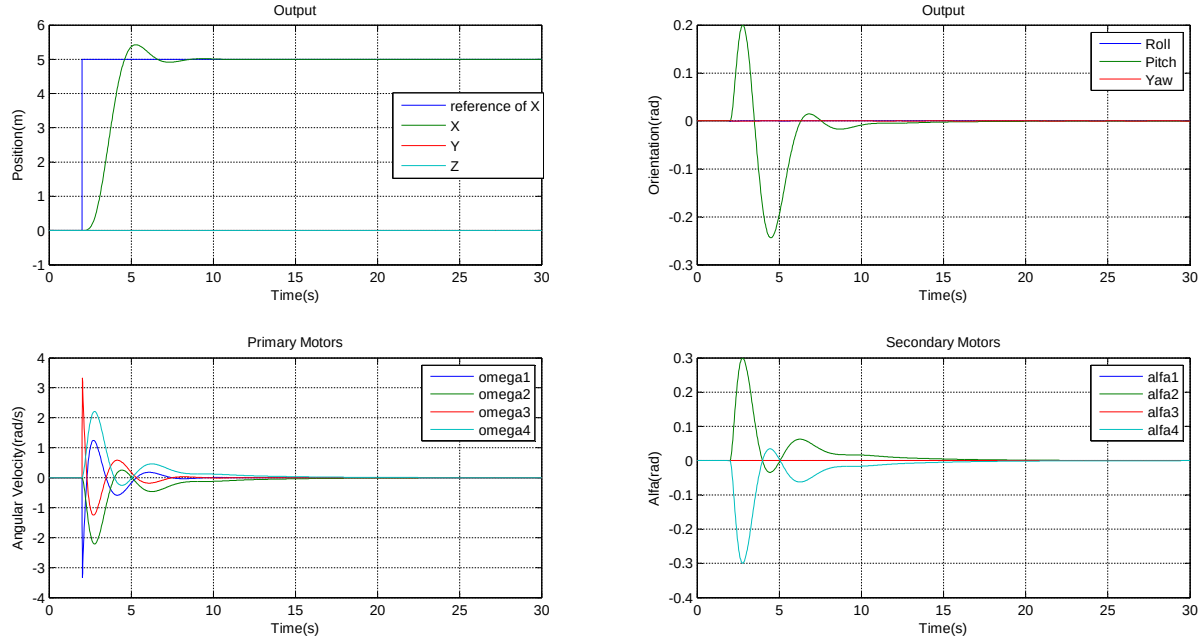

Figure 3.6: Position control of the quad-tiltrotor without any disturbances for operation mode $\beta = 0.5$

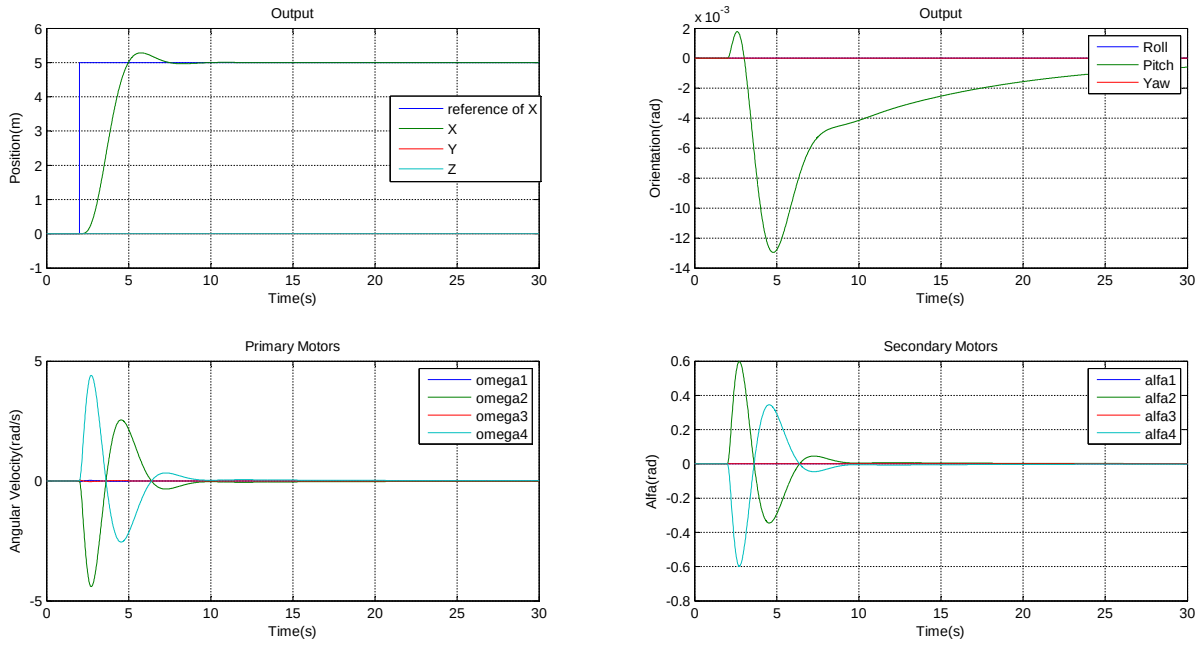

Figure 3.7: Position control of the quad-tiltrotor without any disturbances for operation mode $\beta = 1$

As Figure 3.5 shows, the lateral movement is caused by the difference between the spinning velocity of the primary motors and secondary motors play no role in this movement (their variations are negligible). It means that the quad-tiltrotor has become a conventional quad-rotor.

Figure 3.6 demonstrates that lateral movement occurs due to both spinning velocity of primary motors and effect of secondary motors.

In figure 3.7, one can see that the lateral movement is caused only by the secondary motors. Note that for moving along the X_W direction we need to have positive pitch angle by reducing $\bar{\omega}_1$ and increasing $\bar{\omega}_3$ as illustrated in Figure 3.5, while $\bar{\omega}_2$ and $\bar{\omega}_4$ compensate the gyroscopic effects caused by α_2 and α_4.

Different modes of quad-tilt-rotor under the effect of disturbances

Now, we want to investigate the ability of the controller to reject a disturbance for three aforementioned modes ($\beta = 0$, $\beta = 0.5$, $\beta = 1$). We assume that a wind with constant speed of 10 $\left[\frac{km}{h}\right]$ is introduced to the quad-tiltrotor as a disturbance in the opposite direction of its movement along the X_W. It starts at 10th second and lasts for 7 seconds.The corresponding results are shown in Figures 3.8, 3.9 and 3.10.

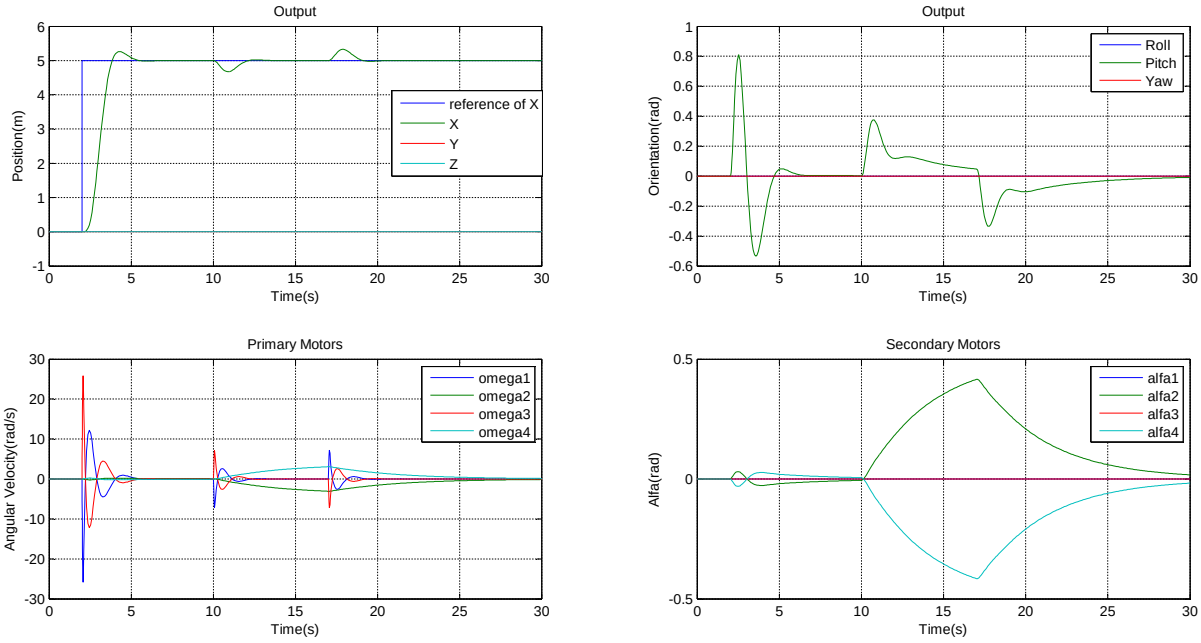

Figure 3.8: Position control of the quad-tiltrotor under the effect of disturbance for operation mode $\beta = 0$

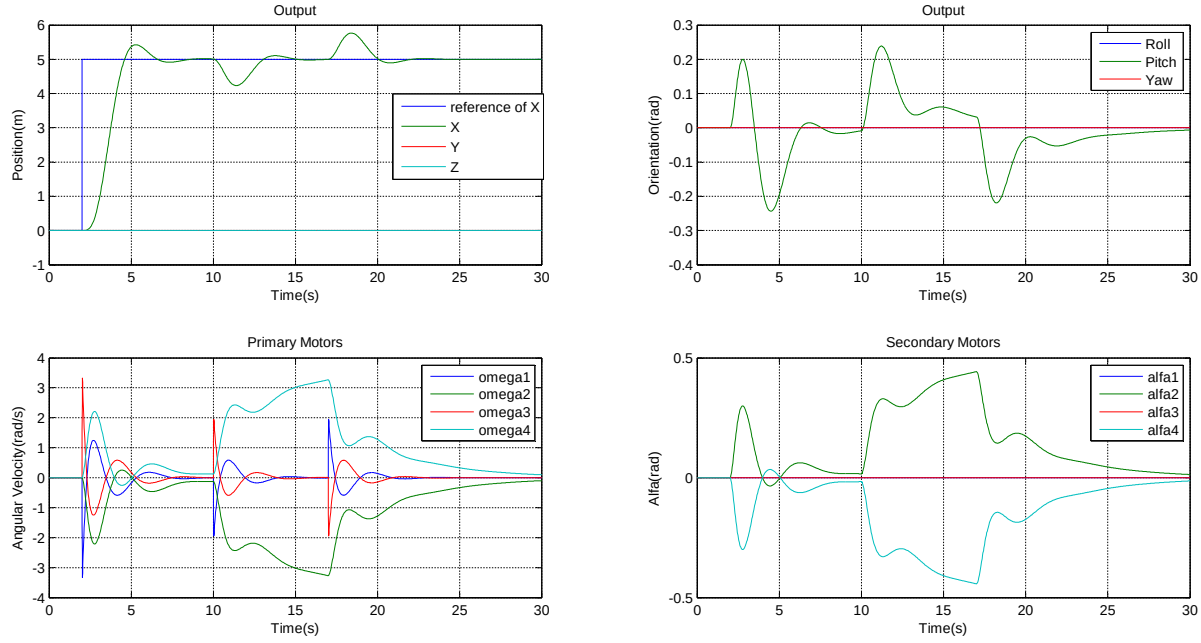

Figure 3.9: Position control of the quad-tiltrotor under the effect of disturbance for operation mode $\beta = 0.5$

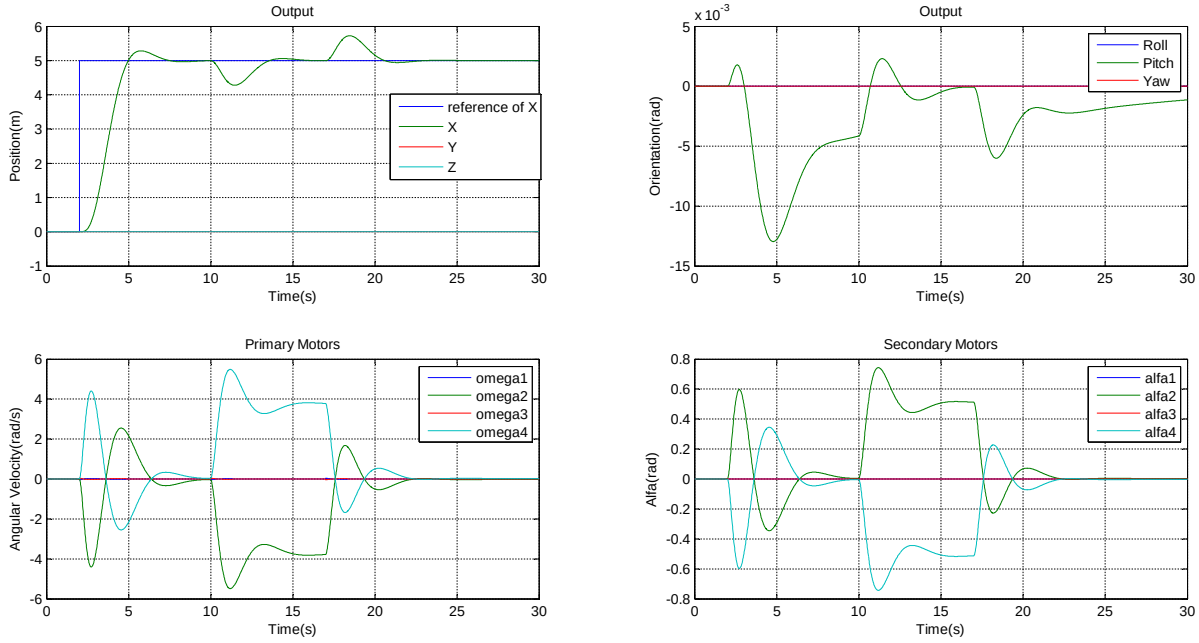

Figure 3.10: Position control of the quad-tiltrotor under the effect of disturbance for operation mode $\beta = 1$

Figure 3.8 shows that in conventional quad-rotor mode, secondary motors help the primary motors for a very fast disturbance rejection.

Figure 3.9 illustrates that when $\beta = 0.5$ the lateral movement caused by the cooperation of the primary and secondary motors. Here, secondary motors help the system to not fully tilt the body.

Figure 3.10 demonstrates that the full quad-tiltrotor is able to overcome the disturbance without tilting the body which this action cannot be done by the conventional quad-rotor.

3.3.2 Attitude control

By choosing proper Q and R matrices (see appendix A) a LQ attitude controller is designed not only to stabilize the system, but also to ensure that the outputs track the reference inputs. In the following figures, the results corresponding to the attitude control of different modes of the quad-tiltrotor, both with and without the effect of disturbances, will be shown.

Different modes of quad-tiltrotor without external disturbances

The quad-tiltrotor is assumed to be at hovering state; after two seconds, position is forced to be at the origin ($X = 0$, $Y = 0$, $Z = 0$) and roll angle equal to 20 degrees ($\phi = 0.35[rad]$). Here, it is supposed that no disturbances affect the system. In Figures 3.11, 3.12 and 3.13, the controller performance for three operation modes of quad-tiltrotor ($\beta = 0$, $\beta = 0.5$, $\beta = 1$), is shown.

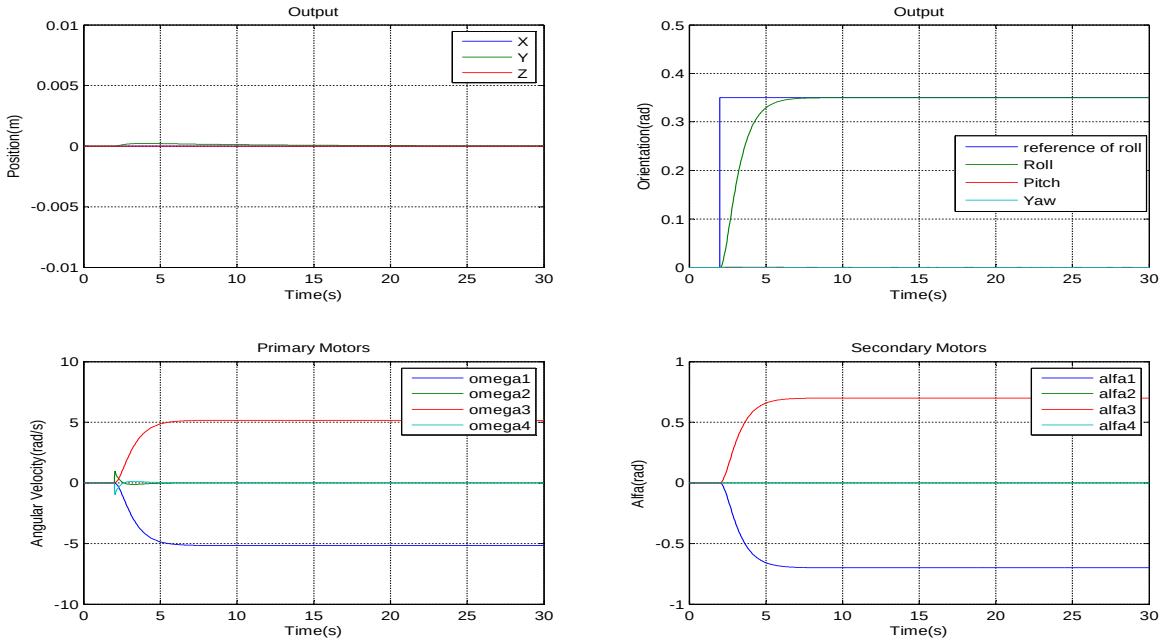

Figure 3.11: Attitude control of the quad-tiltrotor without any disturbances for operation mode $\beta = 0$

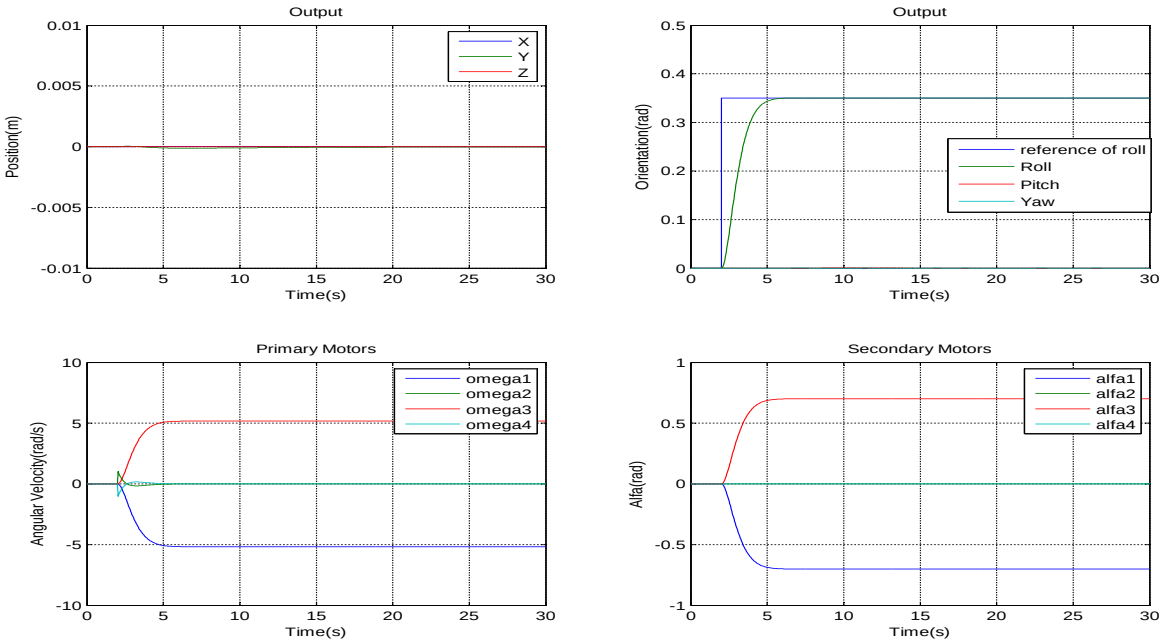

Figure 3.12: Attitude control of the quad-tiltrotor without any disturbances for operation mode $\beta = 0.5$

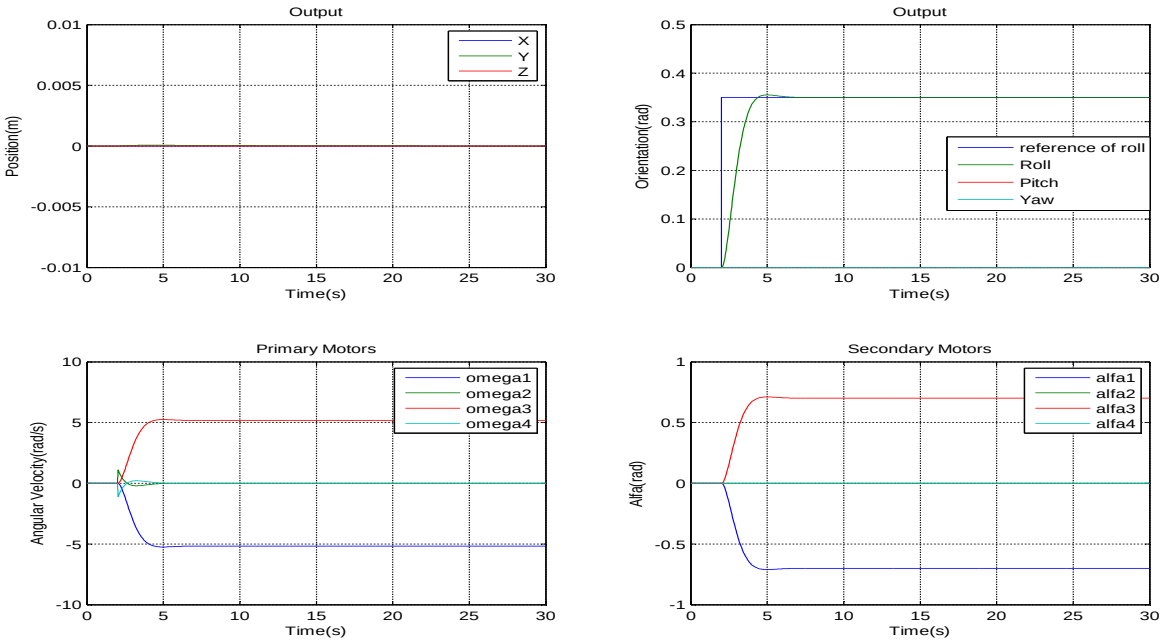

Figure 3.13: Attitude control of the quad-tiltrotor without any disturbances for operation mode $\beta = 1$

Figures 3.11, 3.12 and 3.13 show that there is no difference between different modes of the quad-tiltrotor; Due to the fact that in conventional quad-rotors, orientation changes results in motion along the X, Y directions. Since here we have forced X, Y equal to zero we must have nonzero tilting angles to compensate the movements along the X, Y directions. Therefore, there is no difference between these three modes.

Different modes of quad-tilt-rotor under the effect of disturbances

Now, we want to investigate the ability of the controller to reject a disturbance for three aforementioned modes, ($\beta = 0$, $\beta = 0.5$, $\beta = 1$). We assume that a wind with constant angular velocity of 0.52 $\left[\frac{rad}{s}\right]$ is introduced to the quad-tiltrotor as a disturbance in the opposite direction of its rotation about the X_B. It starts at 10th second and lasts for 7 seconds.

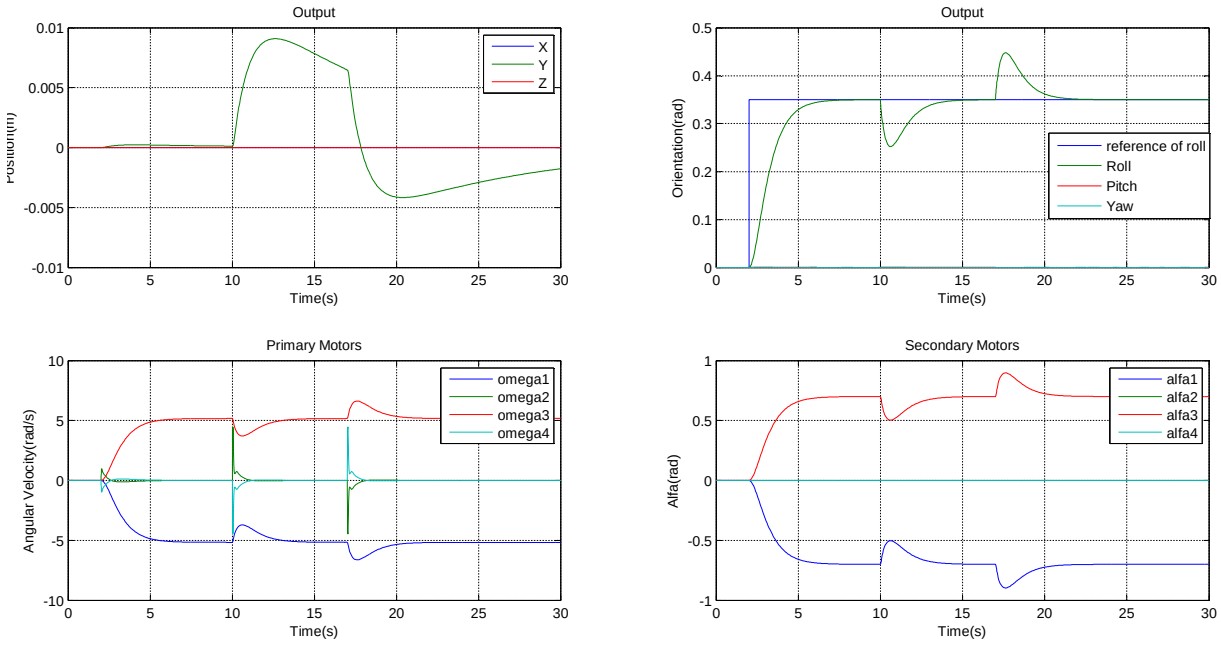

Figure 3.14: Attitude control of the quad-tiltrotor under the effect of disturbance for operation mode $\beta = 0$

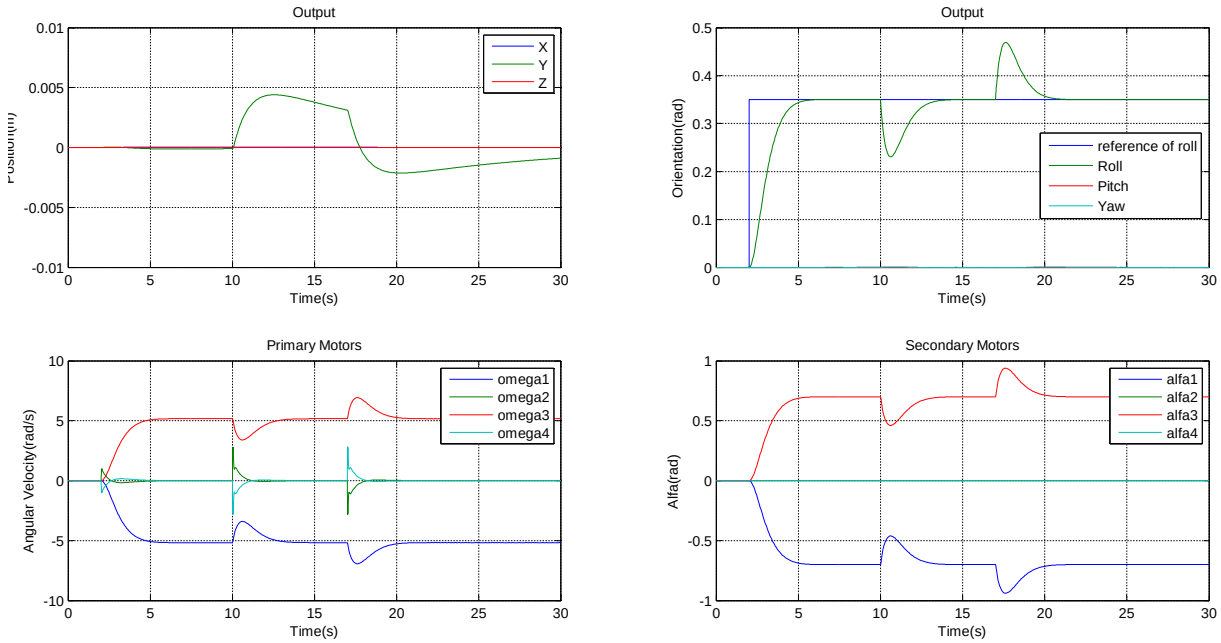

Figure 3.15: Attitude control of the quad-tiltrotor under the effect of disturbance for operation mode $\beta = 0.5$

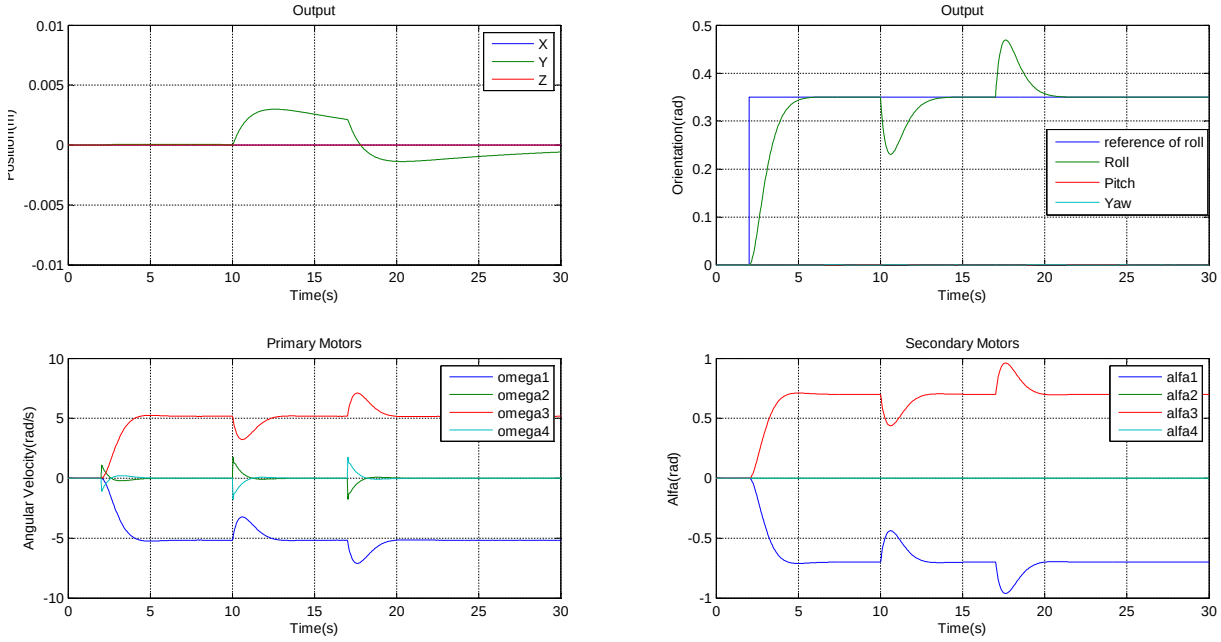

Figure 3.16: Attitude control of the quad-tiltrotor under the effect of disturbance for operation mode $\beta = 1$

According to Figures 3.14, 3.15, 3.16 and analogous with the results obtained in Section 3.3.2, there is no difference between different modes of the quad-tiltrotor in attitude control.

3.4 Optimal H_∞ Control

Consider the following linear system:

$$\begin{aligned} \dot{x}(t) &= Ax(t) + B_1 w(t) + B_2 u(t) \\ z(t) &= C_1 x(t) + D_{12} u(t). \end{aligned} \tag{3.22}$$

Here, $x(t)$, $u(t)$ and $z(t)$ denote the state, the control input, and controlled output vectors. The vector $w(t)$ is the disturbance vector. The matrices A, B_1, C_1, D_{12} and B_2 are matrices of appropriate dimensions. Suppose the state feedback law

$$u(t) = Kx(t) \tag{3.23}$$

is applied to the system. Then the closed-loop system becomes:

$$\begin{aligned} \dot{x}(t) &= (A + B_2 K)x(t) + B_1 w(t) \\ z(t) &= (C_1 + D_{12} K)x(t). \end{aligned} \tag{3.24}$$

The transfer function from w to z is:

$$T_{zw}(s) = (C_1 + D_{12}K)(sI - A - B_2 K)^{-1} B_1. \tag{3.25}$$

Suppose that the influence of the disturbance vector $w(t)$ on the output $z(t)$ is measured by the H_∞-norm of $T_{zw}(s)$. The goal of the state feedback H_∞ control problem is to find a constant feedback matrix K such that the closed-loop system is stable and the H_∞-norm of the transfer matrix $T_{zw}(s)$ is less than a prescribed tolerance γ [26].

When γ is minimum, it is called optimal state feedback H_∞ problem.
Note that the minimum value of γ is not a priori known, and an iterative procedure must be used. In this thesis, the value of γ has been progressively reduced until the minimum value satisfying the previous relation was met. $\|T_{zw}(s)\|_\infty < \gamma$ can be written as:

$$\int_0^\infty (C_1 x(t) + D_{12} u(t))^T (C_1 x(t) + D_{12} u(t)) dt \leq \gamma^2 \int_0^\infty w^T(t) w(t) dt \tag{3.26}$$

or, similar to equation (3.17)

$$\int_0^\infty \begin{bmatrix} x(t) \\ u(t) \end{bmatrix}^T \begin{bmatrix} Q & S \\ S^T & R \end{bmatrix} \begin{bmatrix} x(t) \\ u(t) \end{bmatrix} dt \leq \gamma^2 \int_0^\infty w^T(t)w(t)dt \tag{3.27}$$

where $Q = {C_1}^T C_1$ ($Q = Q^T \geq 0$), $R = {D_{12}}^T D_{12}$ ($R = R^T > 0$) and $S = {C_1}^T D_{12}$.

Theorem 3.4.1. Let pair (A, C_1) be observable and the pairs (A, B_1) and (A, B_2) be stabilizable. Then the H_∞ control problem (as stated above) has a solution if there exists a positive semi-definite solution P of the algebraic Riccati equation

$$\tilde{A}^T P + P\tilde{A} - P(B_2 R^{-1} {B^T}_2 - \frac{1}{\gamma^2} B_1 {B^T}_1)P + \tilde{Q} = 0 \tag{3.28}$$

where $\tilde{A} = A - B_2 R^{-1} S^T$ and $\tilde{Q} = Q - S R^{-1} S^T$ such that $\tilde{A} + (\frac{1}{\gamma^2} B_1 {B^T}_1 + B_2 R^{-1} {B^T}_2)P$ is stable. In this case one such state feedback matrix K is given by

$$K = -R^{-1}(B_2^T P + S^T). \tag{3.29}$$

Remark: to solve the Riccati equation (3.28) by $MATLAB$, one should use built-in function *care*. Therefore, it is required to write the Riccati equation (3.28) in the *care* format as

$$A^T P + PA + (P \begin{bmatrix} B_1 & B_2 \end{bmatrix} + \begin{bmatrix} 0 & S \end{bmatrix}) \begin{bmatrix} -\gamma^2 & 0 \\ 0 & R \end{bmatrix}^{-1} (\begin{bmatrix} B_1^T \\ B_2^T \end{bmatrix} P + \begin{bmatrix} 0 \\ S^T \end{bmatrix}) + Q = 0$$
$$P = care(A, \begin{bmatrix} B_1 & B_2 \end{bmatrix}, Q, \tilde{R}, \begin{bmatrix} 0 & S \end{bmatrix})$$

where $\tilde{R} = \begin{bmatrix} -\gamma^2 & 0 \\ 0 & R \end{bmatrix}$.

Letting $x(0) = 0$, we want to verify that the control law

$$u(t) = -R^{-1}(B_2^T P + S^T)x(t)$$

guarantees the attenuation level γ from w to z, that is

$$\|z\|_2 \leq \gamma \|w\|_2.$$

Consider the function

$$V(t) = x^T(t)Px(t) + \int_0^t (z^T(\tau)z(\tau) - \gamma^2 w^T(\tau)w(\tau))d\tau.$$

It is apparent that, if $V(t) \leq 0$ for any t, the integrand is negative and the prescribed attenuation level is attained. Note preliminarily that $V(0) = 0$, then if $\dot{V}(t) \leq 0$ for any t, V is negative or null at any time [24]. But, removing the dependence on time for readability,

$$\begin{aligned}
\dot{V} &= \dot{x}^T Px + x^T P\dot{x} + z^T z - \gamma^2 w^T w \\
&= (Ax + B_1 w + B_2 u)^T Px + x^T p(Ax + B_1 w + B_2 u) \\
&+ (C_1 x(t) + D_{12} u(t))^T (C_1 x(t) + D_{12} u(t)) - \gamma^2 w^T w \\
&= x^T (A^T P + PA + Q)x + w^T B_1^T Px + u^T B_2^T Px + x^T PB_1 w \\
&+ x^T PB_2 u + x^T Su + u^T S^T x + u^T Ru - \gamma^2 w^T w \\
&= (a)
\end{aligned} \tag{3.30}$$

By summing and subtracting $x^T SR^{-1}B_2^T Px$, $x^T PB_2 R^{-1}S^T x$, $\frac{1}{\gamma^2}x^T PB_1 B_1^T Px$, $x^T PB_2 R^{-1}B_2^T Px$ and $x^T SR^{-1}S^T x$ it is possible to write

$$\begin{aligned}
(a) &= x^T(\tilde{A}^T P + P\tilde{A} - P(B_2 R^{-1}B^T{}_2 - \frac{1}{\gamma^2}B_1 B^T{}_1)P + \tilde{Q})x \\
&+ (u^T + x^T(S + PB_2)R^{-1})R(u + R^{-1}(B_2^T P + S^T)x) \\
&- \gamma^2(w^T - \frac{1}{\gamma^2}x^T PB_1)(w - \frac{1}{\gamma^2}B_1^T Px)
\end{aligned} \tag{3.31}$$

Therefore, if P is computed as the solution of the previous Riccati equation and the control law $u(t) = -R^{-1}(B_2^T P + S^T)x(t)$ is used, one obtaines

$$\dot{V} = -\gamma^2(w^T - \frac{1}{\gamma^2}x^T PB_1)(w - \frac{1}{\gamma^2}B_1^T Px) \leq 0 \tag{3.32}$$

and the result is proven.

In this section, it is assumed that the disturbance affect the linear and angular velocity of the quad-tiltrotor. Then, matrix B_1 and disturbance vector $w(t)$ are as follows

$$B_1 = \begin{bmatrix} 0 & 0 & 0 & 0 & 0 & 0 \\ 1 & 0 & 0 & 0 & 0 & 0 \\ 0 & 0 & 0 & 0 & 0 & 0 \\ 0 & 1 & 0 & 0 & 0 & 0 \\ 0 & 0 & 0 & 0 & 0 & 0 \\ 0 & 0 & 1 & 0 & 0 & 0 \\ 0 & 0 & 0 & 0 & 0 & 0 \\ 0 & 0 & 0 & 1 & 0 & 0 \\ 0 & 0 & 0 & 0 & 0 & 0 \\ 0 & 0 & 0 & 0 & 1 & 0 \\ 0 & 0 & 0 & 0 & 0 & 0 \\ 0 & 0 & 0 & 0 & 0 & 1 \end{bmatrix}$$

$$w(t) = \begin{bmatrix} \ddot{X} & \ddot{Y} & \ddot{Z} & \ddot{\phi} & \ddot{\theta} & \ddot{\psi} \end{bmatrix}^T.$$

The block diagram of the associated control system is shown in Figure 3.17, where $G(s)$ is the system presented in equation (3.5), H_∞ represents the controller designed by H_∞ technique, input β is the operation mode adjustment of the quad-tiltrotor and γ is the performance level of the H_∞ control.

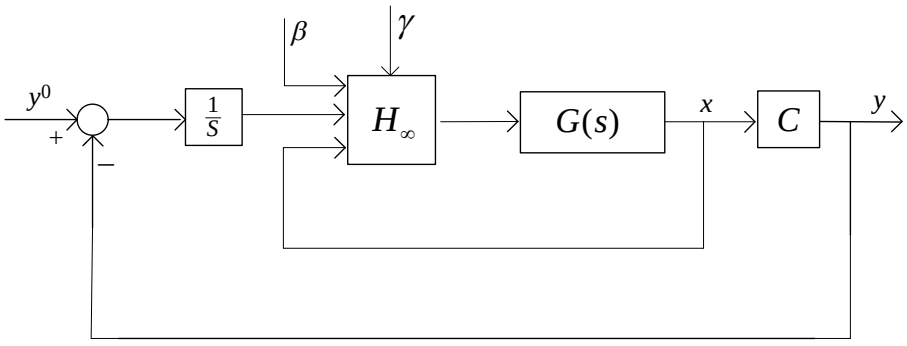

Figure 3.17: Block diagram of the H_∞ control algorithm

The block diagram of the control system is implemented in *Simulink* and required parameters are taken from *MATLAB* workspace. The *Simulink* block diagram of the system is illustrated below in Figure 3.18.

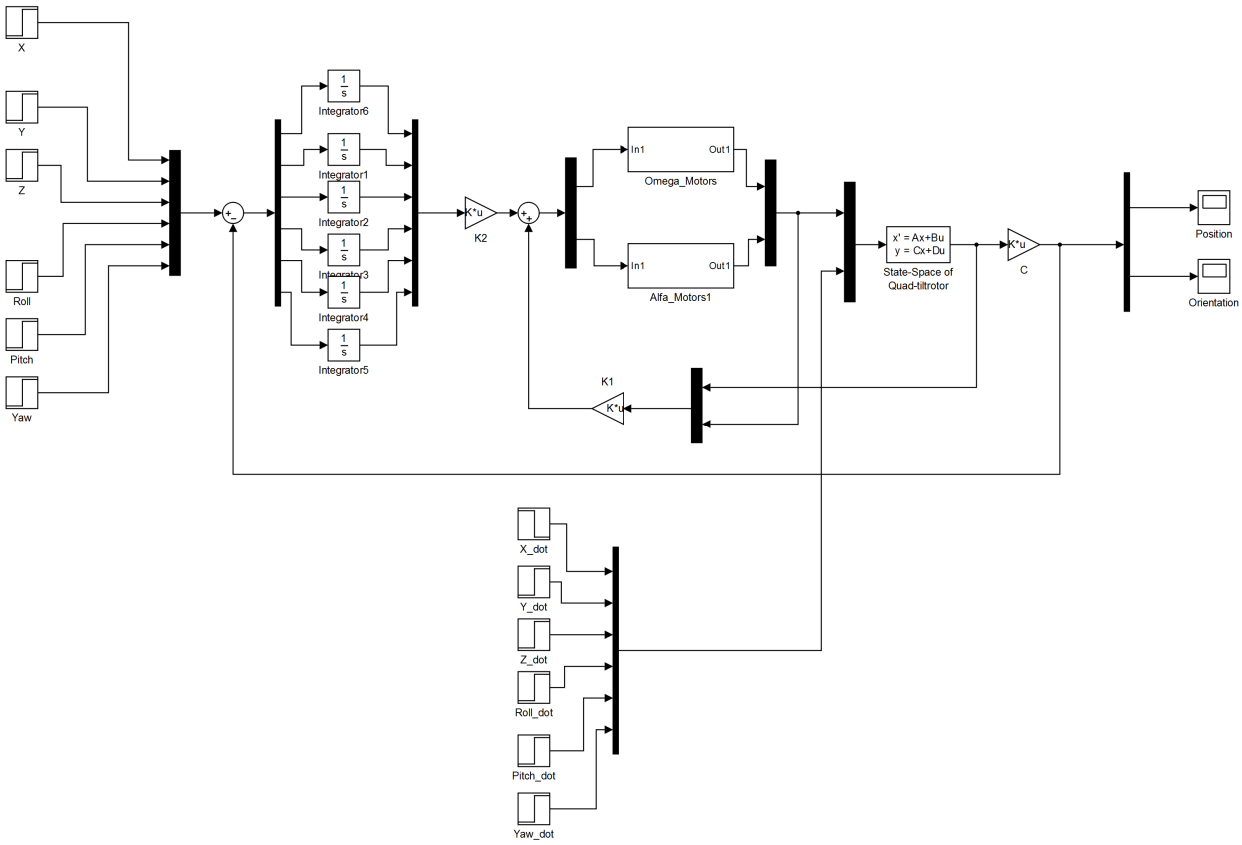

Figure 3.18: Block diagram of the H_∞ control algorithm implemented in *Simulink*

The gain $\bar{K}$ is calculated using *MATLAB* and is separated into K_1 corresponding to the state feedback and K_2 corresponding to the integral gain.

Now, we want to compare the controllers designed by *LQ* technique in Section

3.3 and H_∞ technique for different modes of the quad-tiltrotor, with the same design parameters Q and R matrixes.

3.4.1 Position control

By using the Q and R matrices obtained in Section 3.3, and computing the minimum value of γ, an optimal H_∞ position controller is designed not only to stabilize the system, but also to ensure that the outputs track the reference inputs in the presence of disturbances.

To see the difference between LQ and H_∞ performances better, we assume that a stronger wind is applied to the system. Therefore, a wind with constant speed of 12 $\left[{}^{km}/_{h}\right]$ is introduced to the quad-tiltrotor as a disturbance in the opposite direction of its movement along the X_W. It starts at 10th second and lasts for 7 seconds. Figures 3.19, 3.20 and 3.21 show the difference between controllers performances for three different operation modes of the quad-tiltrotor.

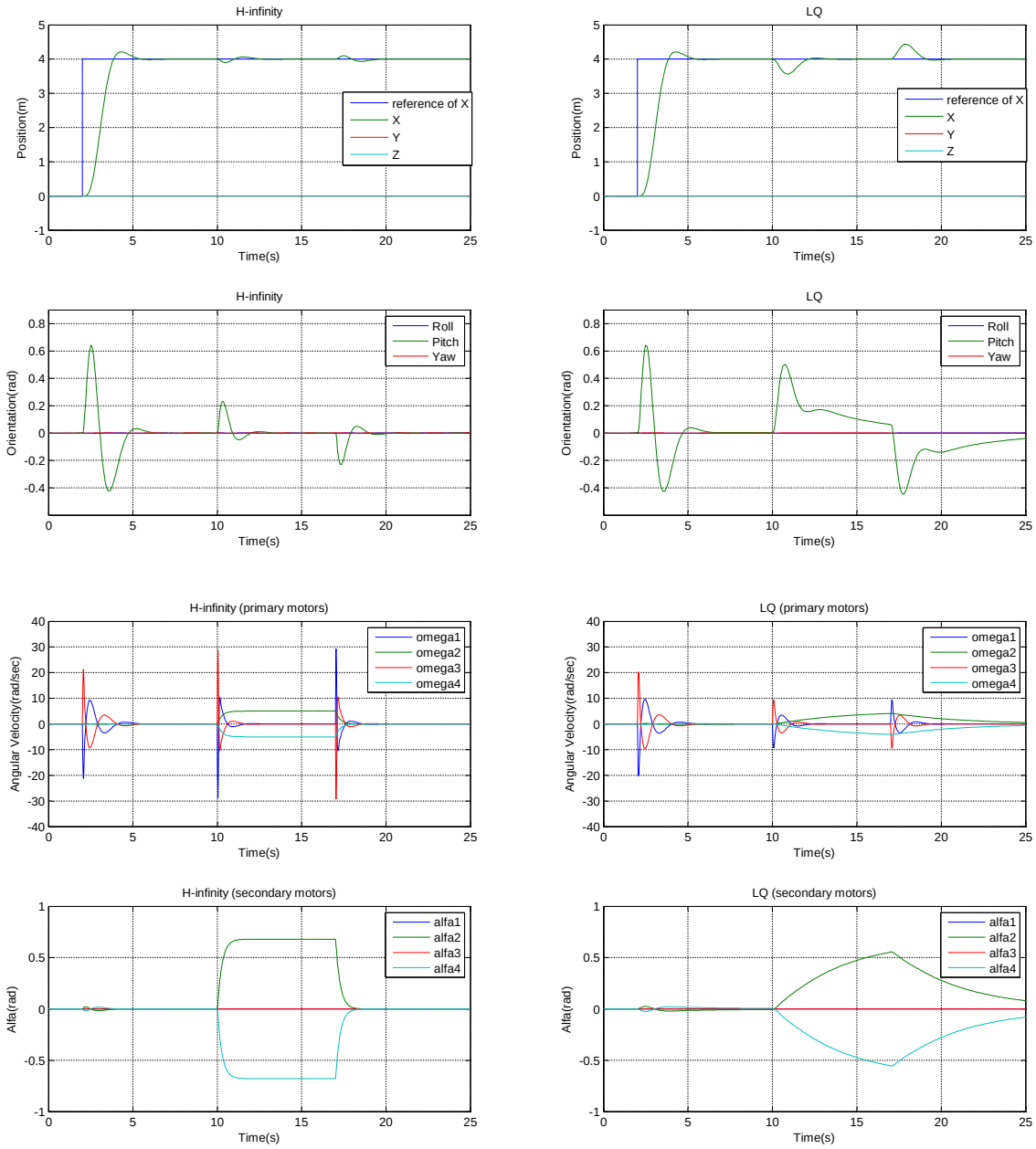

Figure 3.19: Comparison between H_∞ and LQ position control ($\beta = 0$ and $\gamma = 28.9$)

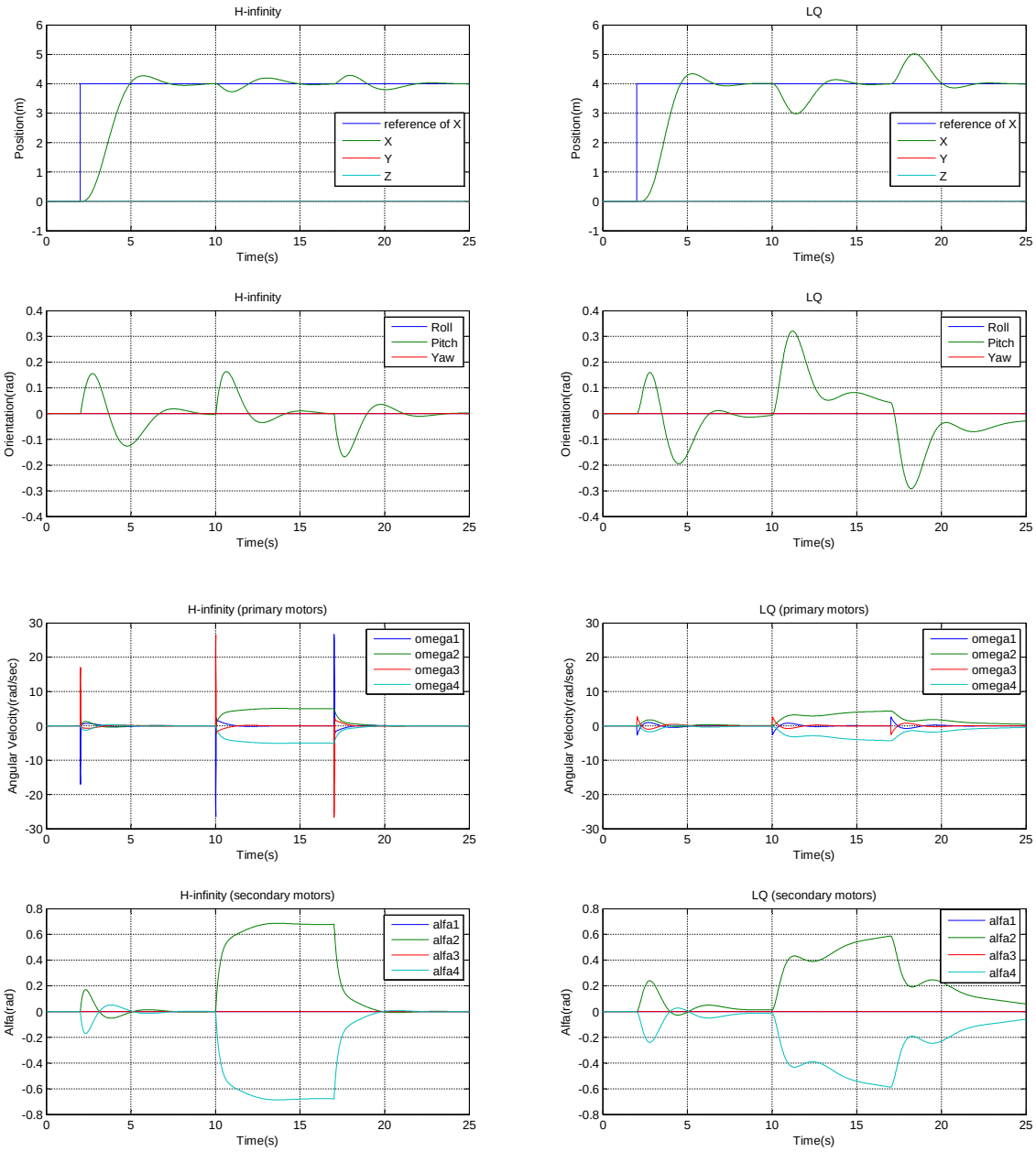

Figure 3.20: Comparison between H_∞ and LQ position control ($\beta = 0.5$ and $\gamma = 28.2$)

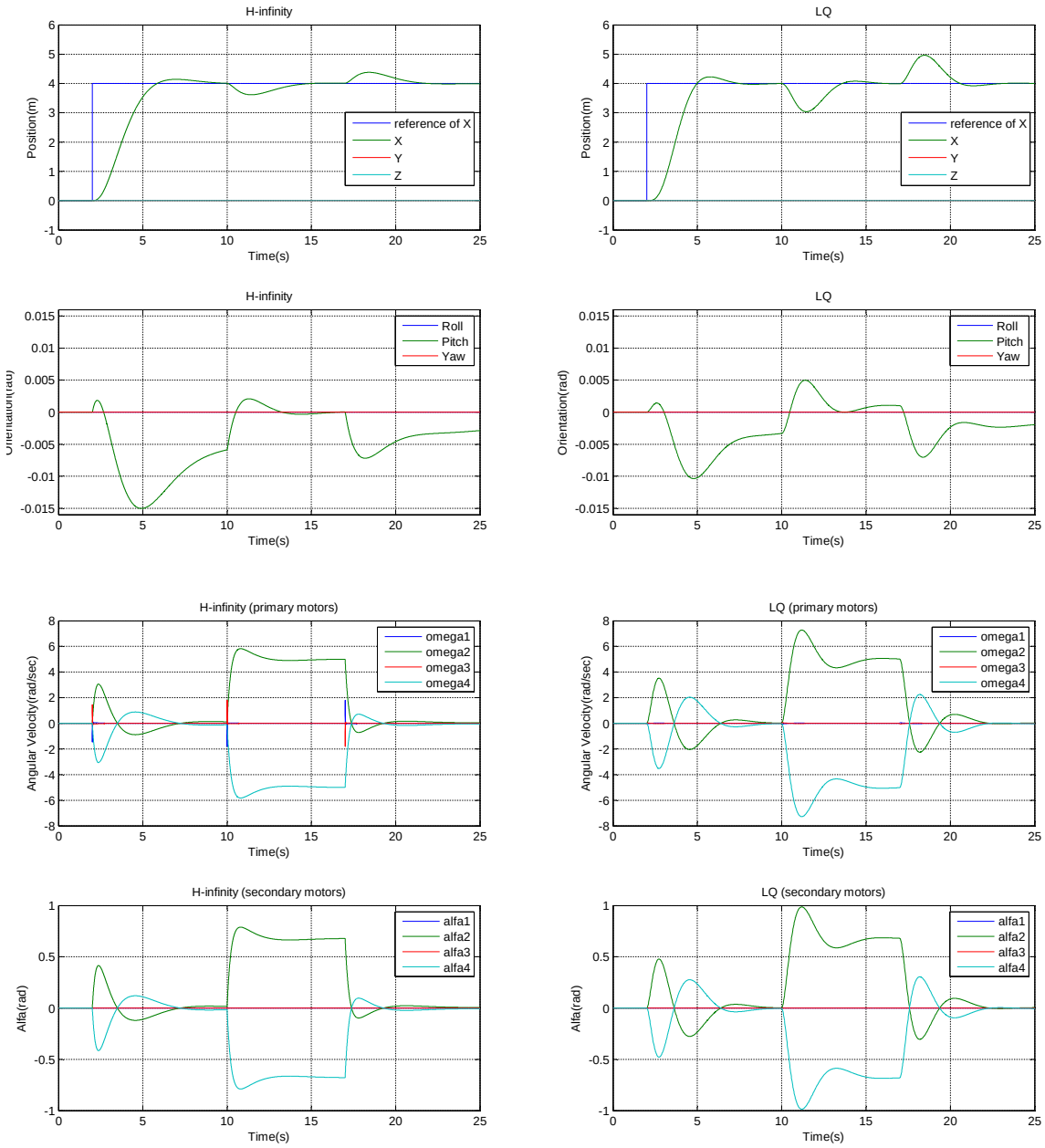

Figure 3.21: Comparison between H_∞ and LQ position control ($\beta = 1$ and $\gamma = 12.4$)

As can be seen in Figures 3.19, 3.20 and 3.21, the system for which a H_∞ controller is designed has a faster response, at the cost of more aggressive control efforts, than the other system. Moreover, the H_∞ controller is more robust against

the disturbances than the LQ controller. These results are true for any modes of the quad-tiltrotor.

3.4.2 Attitude control

By choosing the same Q and R matrixes as selected in Section 3.3, and computing the minimum value of γ, a H_∞ attitude controller is designed not only to stabilize the system but also to ensure that the outputs track the reference inputs in the presence of disturbances.

Here, it is assumed that a wind with constant angular velocity of $0.52 \left[{}^{rad}/_{s} \right]$ is introduced to the quad-tiltrotor as a disturbance in the opposite direction of its rotation about the X_B. It starts at 10th second and lasts for 7 seconds.

In the following Figures 3.22, 3.23 and 3.24, the results correspond to the H_∞ and LQ attitude controllers for the three different operation modes of quad-tiltrotor, are shown.

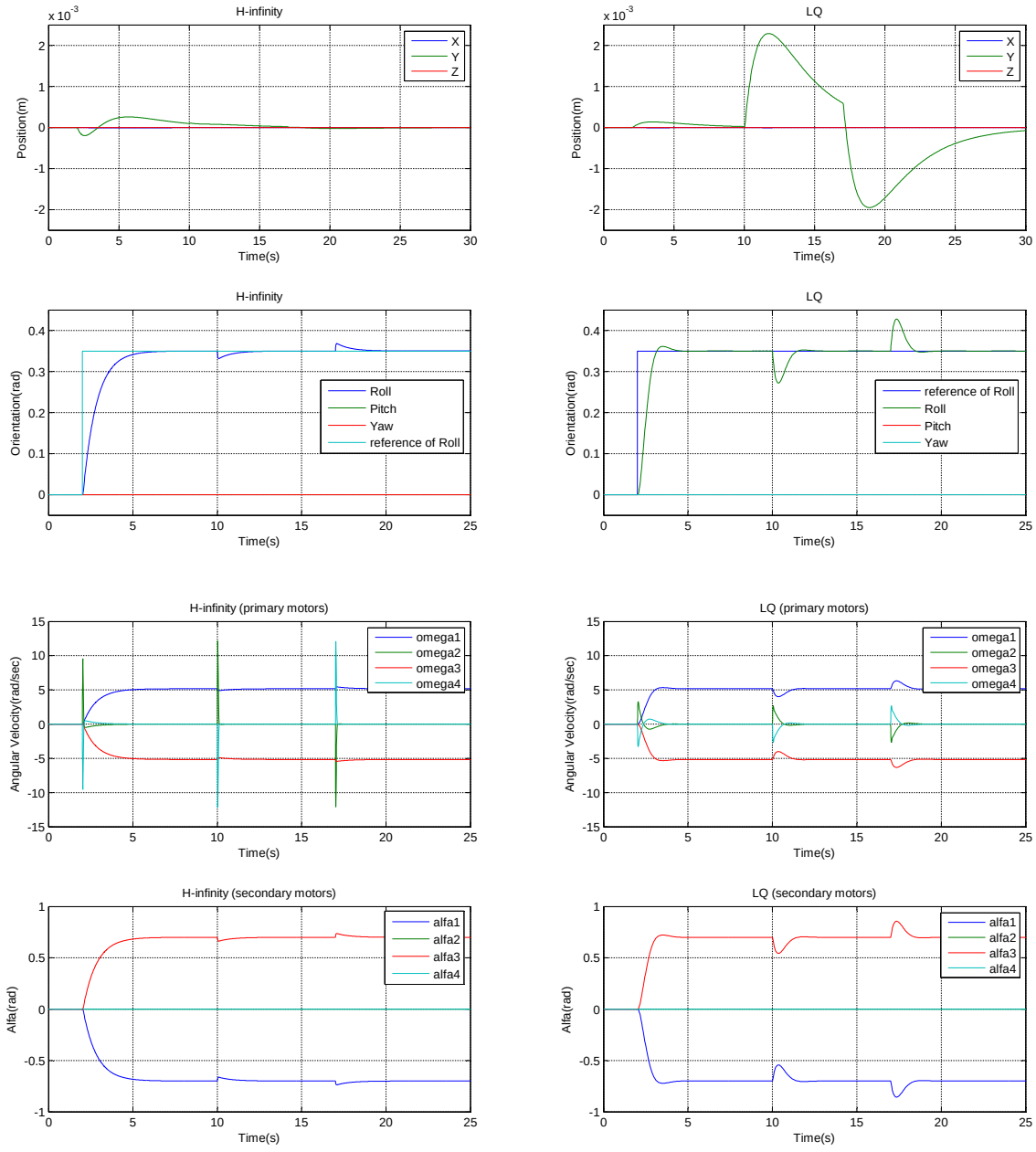

Figure 3.22: Comparison between H_∞ and LQ attitude control ($\beta = 0$ and $\gamma = 10.5$)

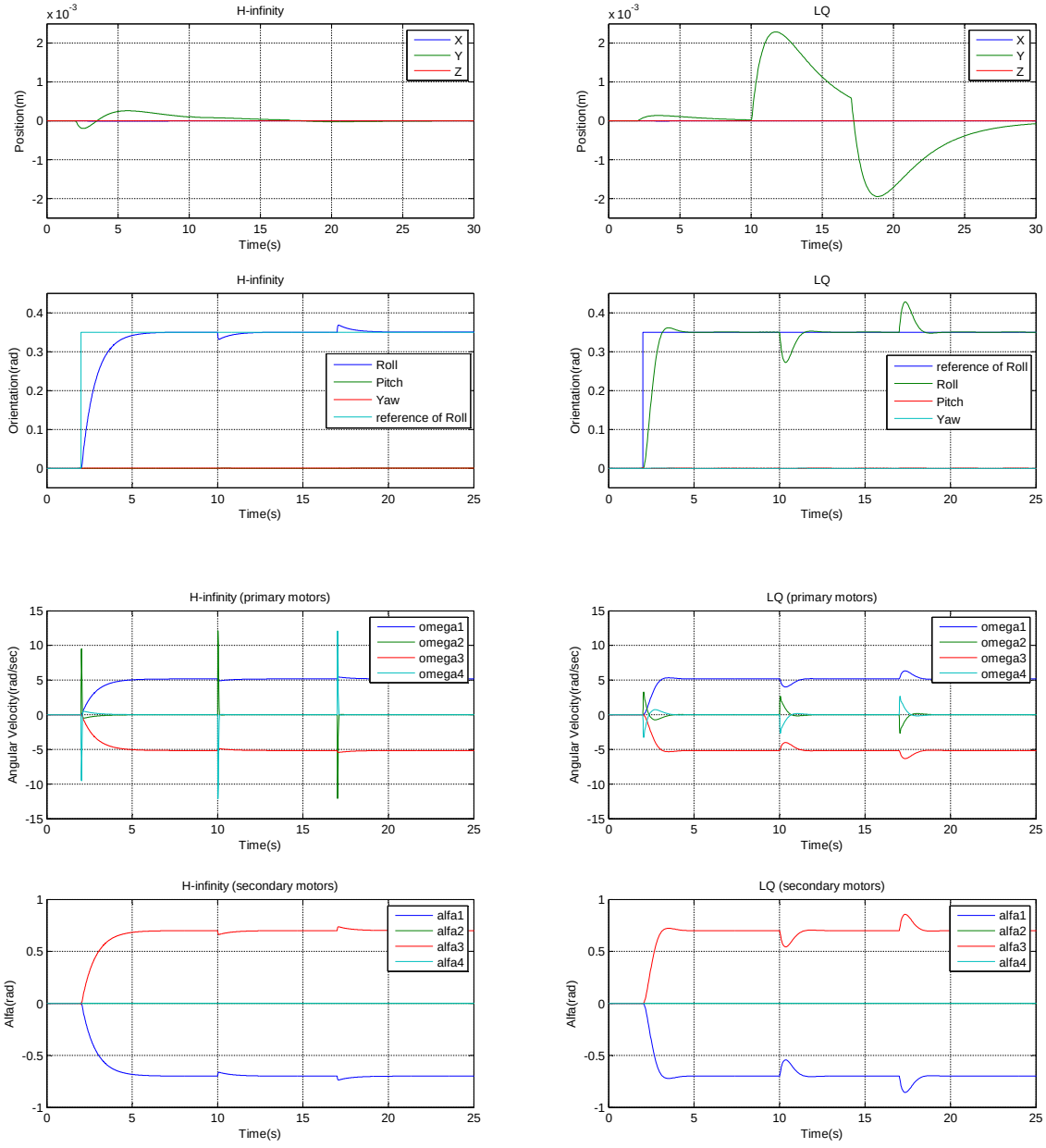

Figure 3.23: Comparison between H_∞ and LQ attitude control ($\beta = 0.5$ and $\gamma = 10.5$)

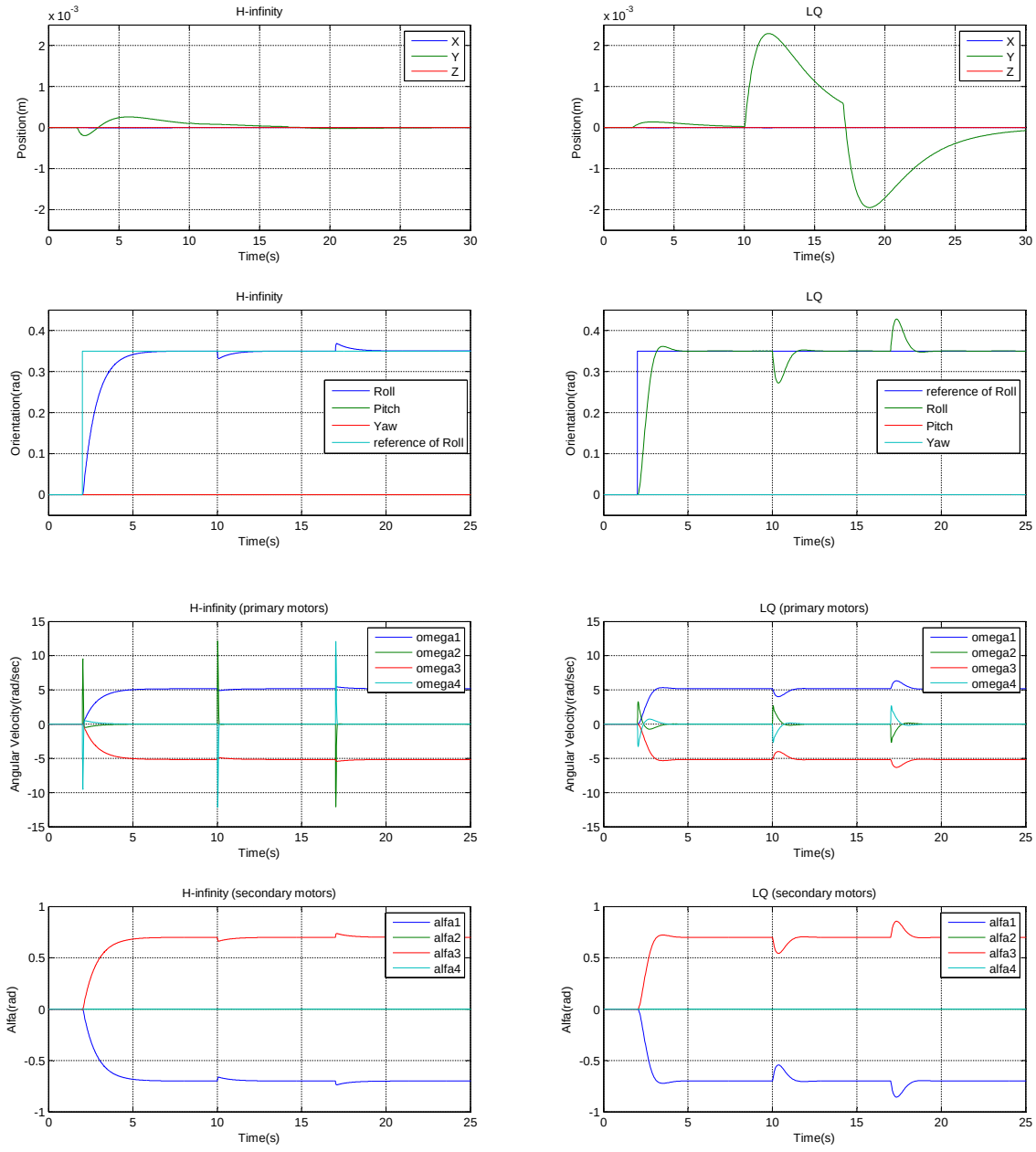

Figure 3.24: Comparison between H_∞ and LQ attitude control ($\beta = 1$ and $\gamma = 10.5$)

Figures 3.22, 3.23 and 3.24 illustrate that the H_∞ controller is more robust against the disturbances than the LQ controller. It is obvious that the H_∞ controller is able to reject the disturbances faster than LQ controller, but one

should note that this advantage results larger control efforts and then more energy consumption. Again, these results are true for any operation modes of the quad-tiltrotor.

3.5 Model uncertainty

Most control designs are based on the use of a design model. The relationship between models and the reality they represent is subtle and complex. A mathematical model provides a map from inputs to responses. The quality of a model depends on how closely its responses match those of the true plant. Since no single fixed model can respond exactly like the true plant, we need, at the very least, a set of maps. However, the modeling problem is much deeper-the universe of mathematical models from which a model set is chosen is distinct from the universe of physical systems. Therefore, a model set that includes the true physical plant can never be constructed. It is necessary for the engineer to make a leap of faith regarding the applicability of a particular design based on a mathematical model. To be practical, a design technique must help make this leap small by accounting for the inevitable inadequacy of models. A good model should be simple enough to facilitate design, yet complex enough to give the engineer confidence that designs based on the model will work on the true plant [27].

The purpose of this section is to verify that how much the model uncertainty can affect the performance of designed controllers. In order to reach this purpose, the following assumptions have been considered.

1. body mass (m) of the quad-tiltrotor varies $\pm 20\%$ around its nominal value
2. propeller thrust coefficient (k_f) varies $\pm 10\%$ around its nominal value
3. propeller drag coefficient (k_m) varies $\pm 10\%$ around its nominal value
4. time constant of primary motors varies $\pm 10\%$ around its nominal value
5. time constant of secondary motors varies $\pm 10\%$ around its nominal value

The aforementioned assumptions are applied to the final model (3.14). The results regarding to the performance of the designed H_∞ and LQ controllers in the presence of the assumed model uncertainties are verified in both position and attitude control problem.

This simulation is repeated for 100 times. As before, the quad-tiltrotor is assumed to be in three modes of operation $\beta = 0$, $\beta = 0.5$, and $\beta = 1$.

3.5.1 Position control

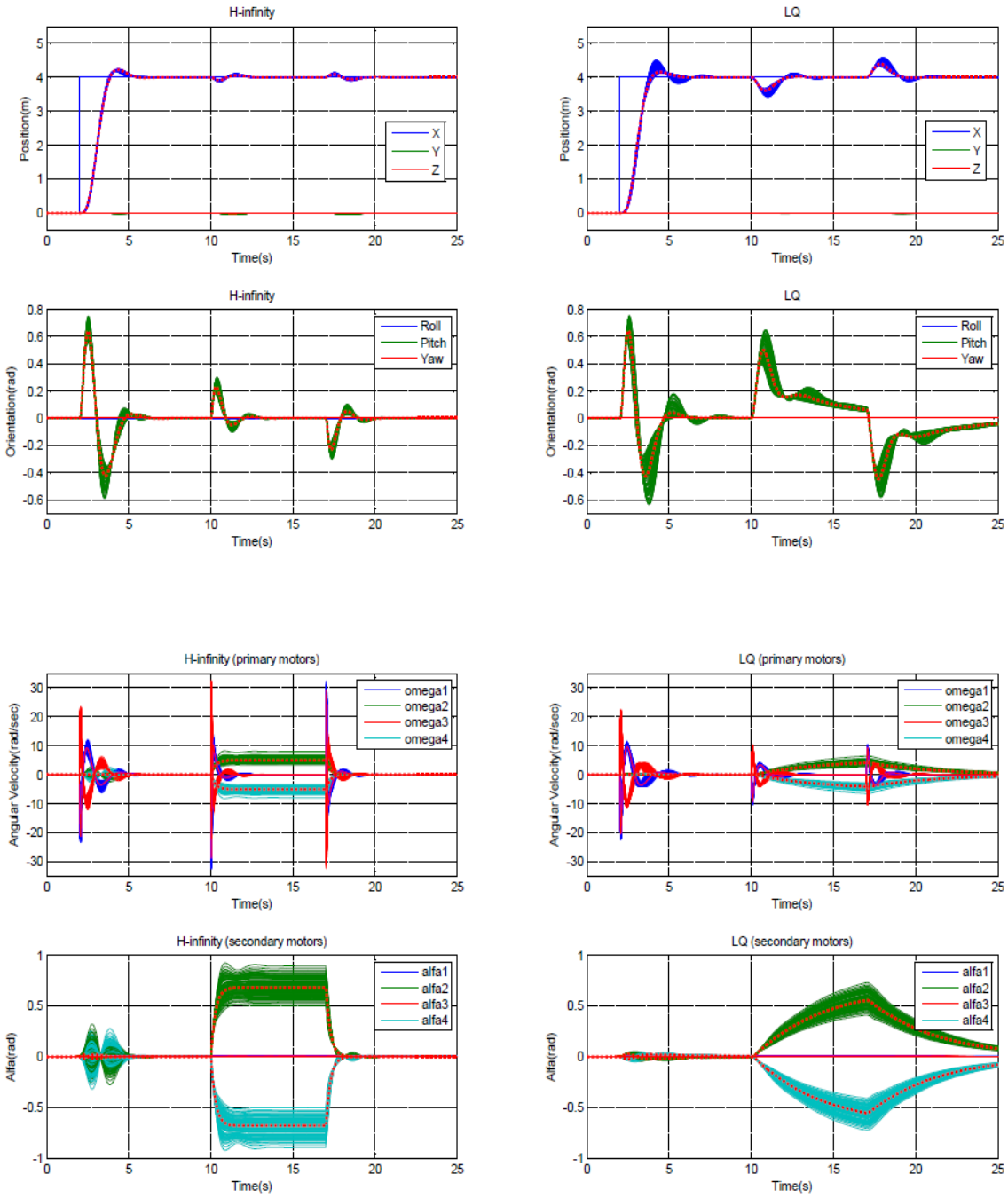

Figure 3.25: Performance of H_∞ and LQ position controllers in presence of model uncertainty. Dashed red lines represent the signals regarding to the nominal values, while solid lines represents the signals regarding to the perturbed model ($\beta = 0$ and $\gamma = 28.9$)

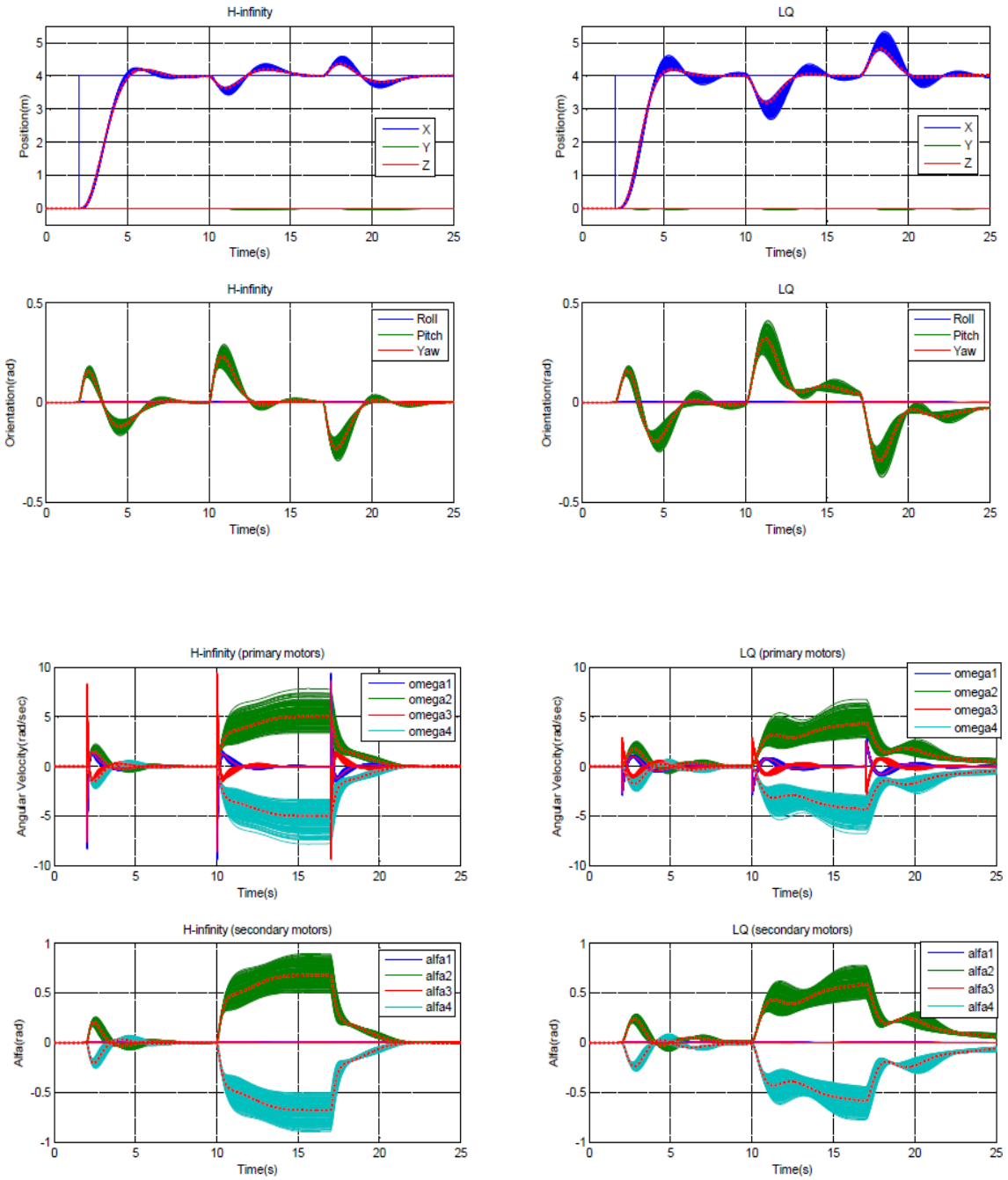

Figure 3.26: Performance of H_∞ and LQ position controllers in presence of model uncertainty. Dashed lines represent the signals regarding to the nominal values, while solid lines represents the signals regarding to the perturbed model ($\beta = 0.5$ and $\gamma = 28.2$)

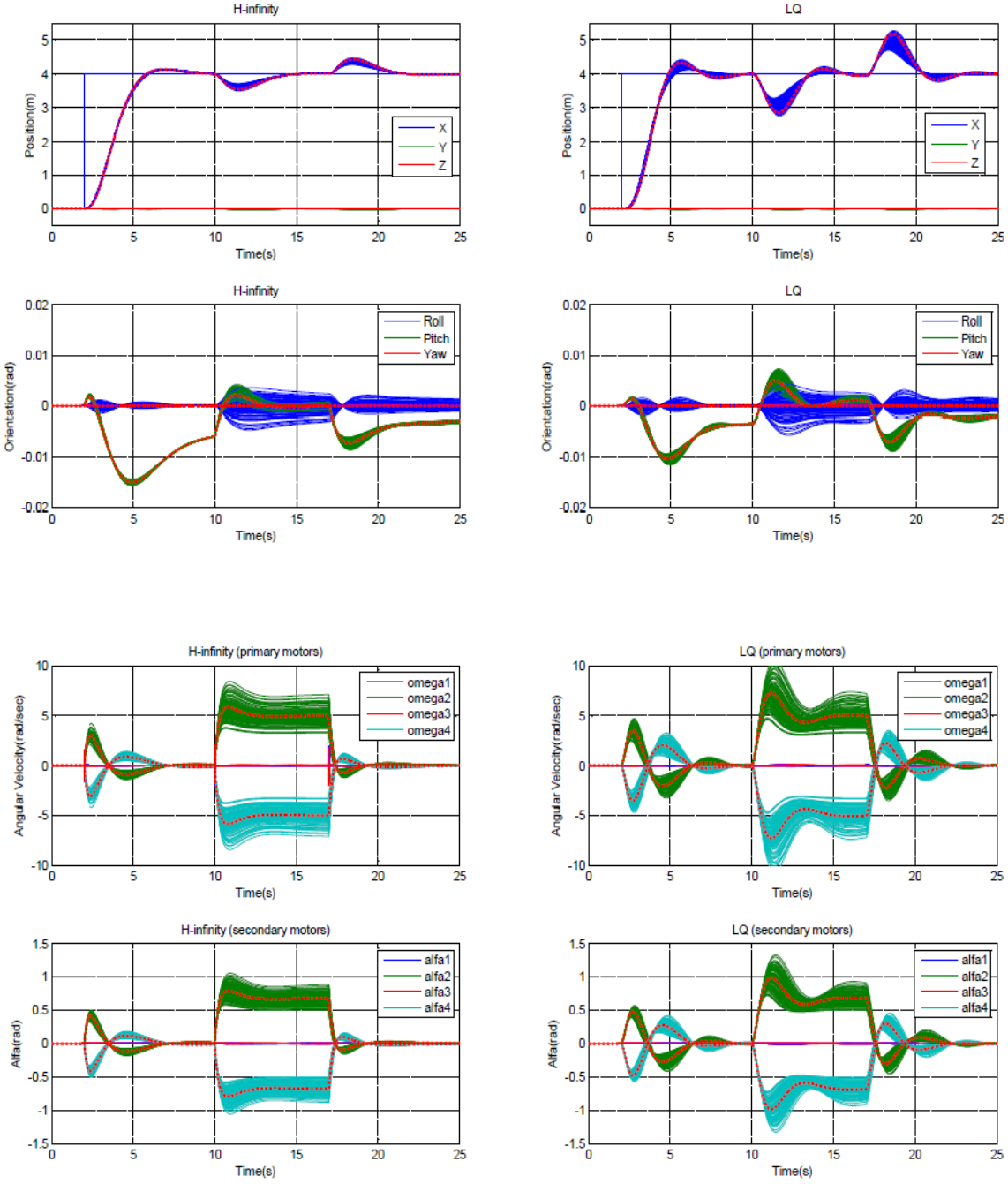

Figure 3.27: Performance of H_∞ and LQ position controllers in presence of model uncertainty. Dashed lines represent the signals regarding to the nominal values, while solid lines represents the signals regarding to the perturbed model ($\beta = 1$ and $\gamma = 12.4$)

3.5.2 Attitude control

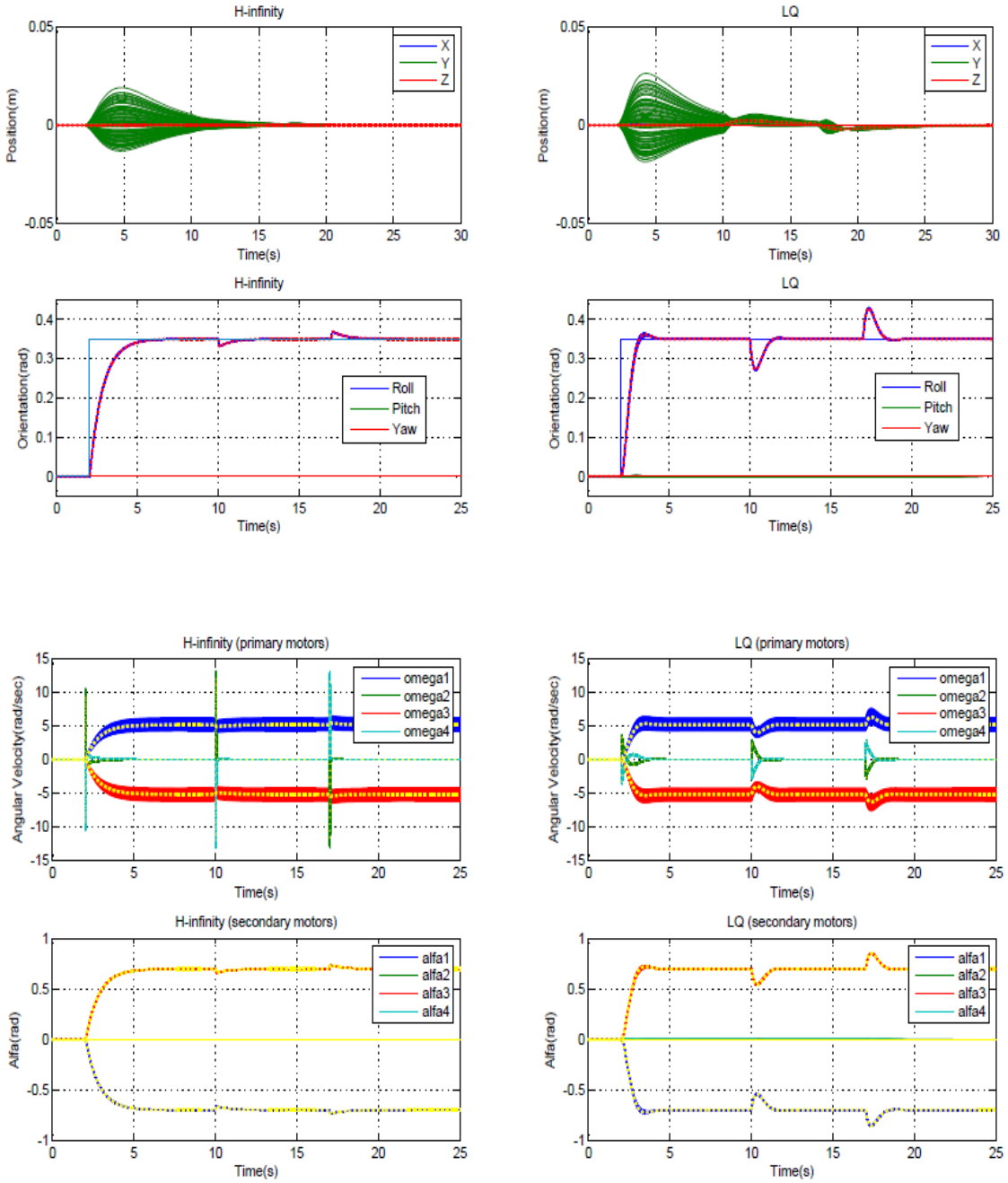

Figure 3.28: Performance of H_∞ and LQ attitude controllers in presence of model uncertainty. Dashed lines represent the signals regarding to the nominal values, while solid lines represents the signals regarding to the perturbed model ($\beta = 0$ and $\gamma = 10.5$)

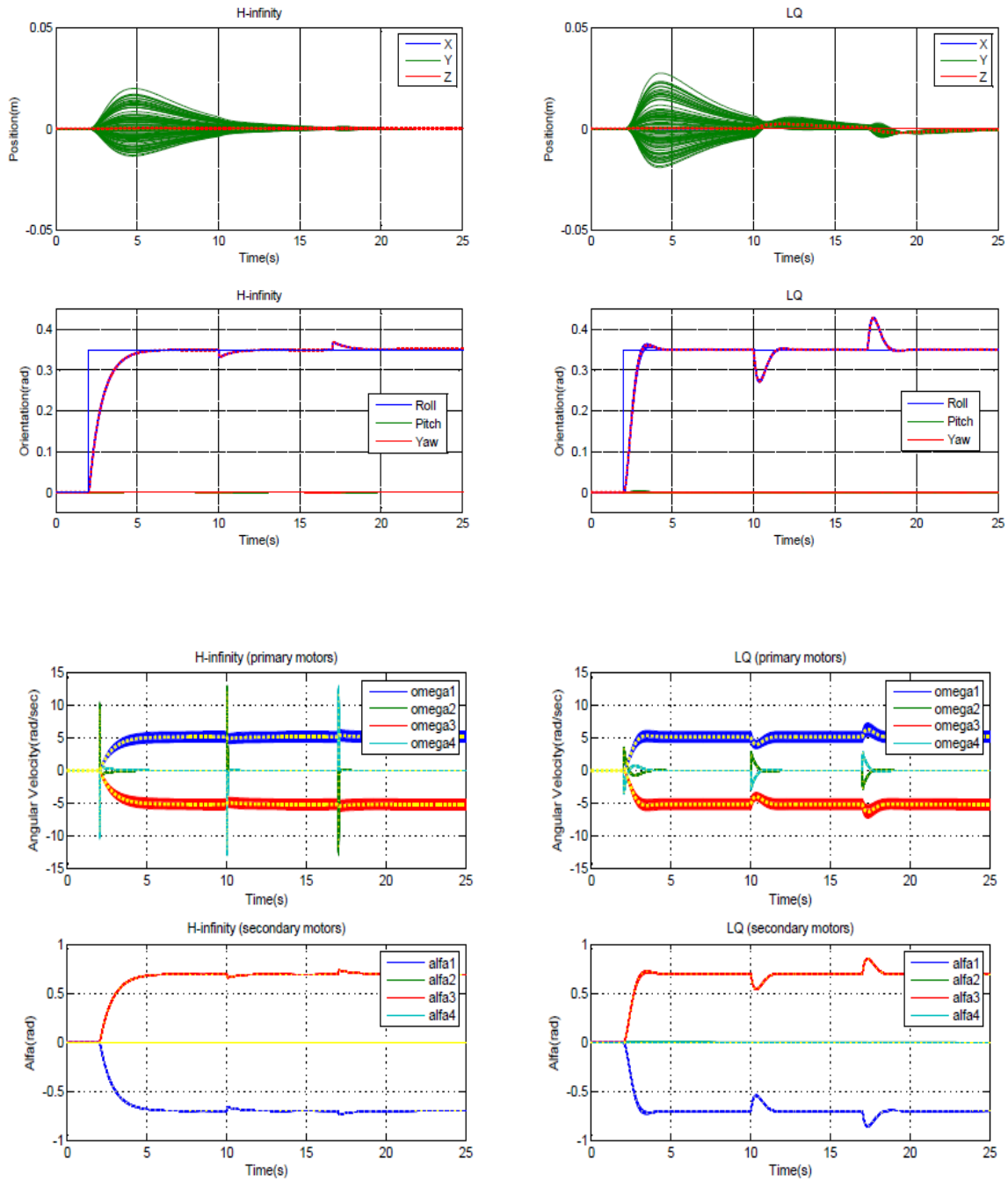

Figure 3.29: Performance of H_∞ and LQ attitude controllers in presence of model uncertainty. Dashed lines represent the signals regarding to the nominal values, while solid lines represents the signals regarding to the perturbed model ($\beta = 0.5$ and $\gamma = 10.5$)

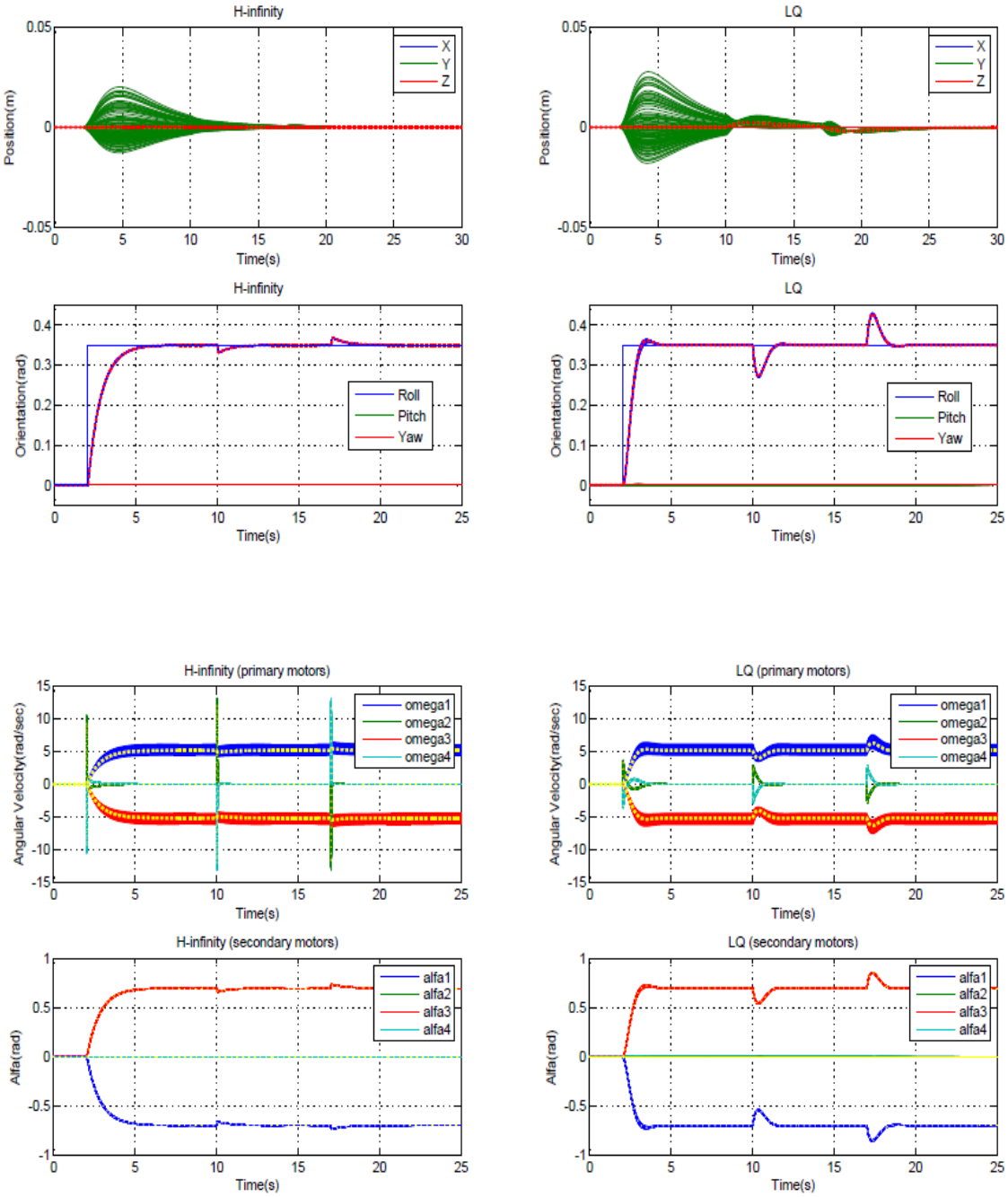

Figure 3.30: Performance of H_∞ and LQ attitude controllers in presence of model uncertainty. Dashed lines represent the signals regarding to the nominal values, while solid lines represents the signals regarding to the perturbed model ($\beta = 1$ and $\gamma = 10.5$)

In this section one can see that in general H_∞ controller has a better performance in both position and attitude control. It has a more robust response than LQ controller.

Chapter 4

Conclusion

In this thesis a new model of quad-rotor has been studied. This new quad-rotor is called quad-tiltrotor and equipped with four extra motors, with respect to quad-rotors, to tilt the propellers. Indeed, the additional set of four control inputs actuating the propeller tilting angles is used to yield full actuation to the quad-rotor position/orientation in space, thus allowing it to behave as a fully actuated flying vehicle. Thanks to Newton-Euler formulation a comprehensive and accurate mathematical model was developed. Then, some simplifications were done to transfer the complicated model to a model more suited to control design. To simplify the full dynamic model, we have neglected the internal gyroscopic/inertial effects by considering them as second-order disturbances to be rejected by the controller. Moreover, the effect of inertia matrix of propellers on the dynamic model was ignored.

Since the purpose of this thesis was to design linear controllers, the nonlinear model already obtained was linearized around hovering state and then transferred to the state-space model ready for designing the controllers. In the next step, model of actuators which contain 4 DC motors for producing spinning velocities and 4 other DC motors to tilt the propellers, were obtained. In this thesis, an adjustable parameter β was introduced to enable us to choose a desired operation mode of quad-tiltrotor between conventional quad-rotor ($\beta = 0$) and full quad-tillrotor ($\beta = 1$) dynamically.

Afterward, two optimal controllers (LQ and H_∞) were developed to control the position and attitude of the quad-tiltrotor in a desired mode. These controllers are designed not only to stabilize the system, but also to ensure that the outputs track the reference inputs in the presence of disturbances.

The simulation results regarding to the LQ controller, proved that this new configuration of aerial vehicle, unlike the conventional quad-rotors, is able to stay in a desired position and orientation simultaneously and remain there in presence of disturbances like wind.

Finally, results regarding to the H_∞ controller showed that this controller is able to reject the disturbances faster than LQ controller but at the cost of larger control inputs and energy consumption. In addition H_∞ controller is more robust than LQ controller against the disturbances.

Appendices

.1 Appendix A

$A =$

Columns 1 through 10

0	1.0000	0	0	0	0	0	0	0	0
0	0	0	0	0	0	0	0	8.4276	0
0	0	0	1.0000	0	0	0	0	0	0
0	0	0	0	0	0	-8.4276	0	0	0
0	0	0	0	0	1.0000	0	0	0	0
0	0	0	0	0	0	0	0	0	0
0	0	0	0	0	0	0	1.0000	0	0
0	0	0	0	0	0	0	0	0	0
0	0	0	0	0	0	0	0	0	1.0000
0	0	0	0	0	0	0	0	0	0
0	0	0	0	0	0	0	0	0	0
0	0	0	0	0	0	0	0	0	0

Columns 11 through 12

0	0
0	0
0	0
0	0
0	0
0	0
0	0
0	0
0	0
0	0
0	1.0000
0	0

$B =$

0	0	0	0	0	0	0	0
0	0	0	0	0	2.1069	0	-2.1069
0	0	0	0	0	0	0	0
0	0	0	0	-2.1069	0	2.1069	0
0	0	0	0	0	0	0	0
0.0093	-0.0093	0.0093	-0.0093	0	0	0	0
0	0	0	0	0	0	0	0
0	-0.4551	0	0.4551	0	3.4270	0	-3.4270
0	0	0	0	0	0	0	0
-0.4551	0	0.4551	0	3.4270	0	-3.4270	0
0	0	0	0	0	0	0	0
-0.0088	-0.0088	-0.0088	-0.0088	-60.6997	-60.6997	-60.6997	-60.6997

$C =$

1	0	0	0	0	0	0	0	0	0	0	0
0	0	1	0	0	0	0	0	0	0	0	0
0	0	0	0	1	0	0	0	0	0	0	0
0	0	0	0	0	0	1	0	0	0	0	0
0	0	0	0	0	0	0	0	1	0	0	0
0	0	0	0	0	0	0	0	0	0	1	0

$A_a =$

```
Columns 1 through 10

         0    1.0000         0         0         0         0         0         0         0         0
         0         0         0         0         0         0         0         0    8.4276         0
         0         0         0    1.0000         0         0         0         0         0         0
         0         0         0         0         0         0   -8.4276         0         0         0
         0         0         0         0         0    1.0000         0         0         0         0
         0         0         0         0         0         0         0         0         0         0
         0         0         0         0         0         0         0    1.0000         0         0
         0         0         0         0         0         0         0         0         0         0
         0         0         0         0         0         0         0         0         0    1.0000
         0         0         0         0         0         0         0         0         0         0
         0         0         0         0         0         0         0         0         0         0
         0         0         0         0         0         0         0         0         0         0
         0         0         0         0         0         0         0         0         0         0
         0         0         0         0         0         0         0         0         0         0
         0         0         0         0         0         0         0         0         0         0
         0         0         0         0         0         0         0         0         0         0
         0         0         0         0         0         0         0         0         0         0
         0         0         0         0         0         0         0         0         0         0
         0         0         0         0         0         0         0         0         0         0
         0         0         0         0         0         0         0         0         0         0



Columns 11 through 20

         0         0         0         0         0         0         0         0         0         0
         0         0         0         0         0         0         0    2.1069         0   -2.1069
         0         0         0         0         0         0         0         0         0         0
         0         0         0         0         0         0   -2.1069         0    2.1069         0
         0         0         0         0         0         0         0         0         0         0
         0         0    0.0093   -0.0093    0.0093   -0.0093         0         0         0         0
         0         0         0         0         0         0         0         0         0         0
         0         0         0   -0.4551         0    0.4551         0    3.4270         0   -3.4270
         0         0         0         0         0         0         0         0         0         0
         0         0   -0.4551         0    0.4551         0    3.4270         0   -3.4270         0
         0    1.0000         0         0         0         0         0         0         0         0
         0         0   -0.0088   -0.0088   -0.0088   -0.0088  -60.6997  -60.6997  -60.6997  -60.6997
         0         0   -8.0000         0         0         0         0         0         0         0
         0         0         0   -8.0000         0         0         0         0         0         0
         0         0         0         0   -8.0000         0         0         0         0         0
         0         0         0         0         0   -8.0000         0         0         0         0
         0         0         0         0         0         0   -4.0000         0         0         0
         0         0         0         0         0         0         0   -4.0000         0         0
         0         0         0         0         0         0         0         0   -4.0000         0
         0         0         0         0         0         0         0         0         0   -4.0000
```

$B_a =$

```
     0     0     0     0     0     0     0     0
     0     0     0     0     0     0     0     0
     0     0     0     0     0     0     0     0
     0     0     0     0     0     0     0     0
     0     0     0     0     0     0     0     0
     0     0     0     0     0     0     0     0
     0     0     0     0     0     0     0     0
     0     0     0     0     0     0     0     0
     0     0     0     0     0     0     0     0
     0     0     0     0     0     0     0     0
     0     0     0     0     0     0     0     0
     0     0     0     0     0     0     0     0
     0     0     0     0     0     0     0     0
     8     0     0     0     0     0     0     0
     0     8     0     0     0     0     0     0
     0     0     8     0     0     0     0     0
     0     0     0     8     0     0     0     0
     0     0     0     0     4     0     0     0
     0     0     0     0     0     4     0     0
     0     0     0     0     0     0     4     0
     0     0     0     0     0     0     0     4
```

$C_a =$

```
Columns 1 through 10

     1     0     0     0     0     0     0     0     0     0
     0     0     1     0     0     0     0     0     0     0
     0     0     0     0     1     0     0     0     0     0
     0     0     0     0     0     0     1     0     0     0
     0     0     0     0     0     0     0     0     1     0
     0     0     0     0     0     0     0     0     0     0

Columns 11 through 20

     0     0     0     0     0     0     0     0     0     0
     0     0     0     0     0     0     0     0     0     0
     0     0     0     0     0     0     0     0     0     0
     0     0     0     0     0     0     0     0     0     0
     0     0     0     0     0     0     0     0     0     0
     1     0     0     0     0     0     0     0     0     0
```

LQ position control

$$Q_\omega = diag(\begin{bmatrix} 100 & 100 & 100 & 100 & 100 & 100 & 100 & 100 & 100 & ... \\ 100 & 100 & 100 & 0.0001 & 0.0001 & 0.0001 & 0.0001 & 0.0001 & 0.0001 & ... \\ 0.0001 & 0.0001 & 5000 & 5000 & 5000 & 5000 & 5000 & 5000 & & \end{bmatrix}).$$

Note: Q_ω is a 26×26 matrix.

$$R_\omega = diag(\begin{bmatrix} 10000 & 10000 & 10000 & 10000 & 0.001 & 0.001 & 0.001 & 0.001 \end{bmatrix}).$$

Note: R_ω is a 8×8 matrix.

$$Q_\alpha = diag(\begin{bmatrix} 100 & 100 & 100 & 100 & 100 & 100 & 100000 & 100000 & ... \\ 100000 & 100000 & 100000 & 100000 & 0.0001 & 0.0001 & 0.0001 & 0.0001 & ... \\ 0.0001 & 0.0001 & 0.0001 & 0.0001 & 1000 & 1000 & 1000 & 1000 & ... \\ 1000 & 1000 & & & & & & & \end{bmatrix}).$$

Again Q_α is a 26×26 matrix.

$$R_\alpha = diag(\begin{bmatrix} 1000 & 1000 & 1000 & 1000 & 0.001 & 0.001 & 0.001 & 0.001 \end{bmatrix}).$$

Again R_α is a 8×8 matrix.

LQ attitude control

$$Q_\omega = diag(\begin{bmatrix} 100000 & 100000 & 100000 & 100000 & 100000 & 100000 & 100 & ... \\ 100 & 100 & 100 & 100 & 100 & 0.0001 & 0.0001 & ... \\ 0.0001 & 0.0001 & 0.0001 & 0.0001 & 0.0001 & 0.0001 & 10000 & ... \\ 10000 & 10000 & 10000 & 10000 & 10000 & & & \end{bmatrix}).$$

Note: Q_ω is a 26×26 matrix.

$$R_\omega = diag(\begin{bmatrix} 0.0001 & 0.0001 & 0.0001 & 0.0001 & 10 & 10 & 10 & 10 \end{bmatrix}).$$

Note: R_ω is a 8×8 matrix.

$$Q_\alpha = diag(\begin{bmatrix} 100000 & 100000 & 100000 & 100000 & 100000 & 100000 & 100 & ... \\ 100 & 100 & 100 & 100 & 100 & 0.0001 & 0.0001 & ... \\ 0.0001 & 0.0001 & 0.0001 & 0.0001 & 0.0001 & 0.0001 & 10000 & ... \\ 10000 & 10000 & 10000 & 10000 & 10000 & & & \end{bmatrix}).$$

Again Q_α is a 26×26 matrix.

$$R_\alpha = diag(\begin{bmatrix} 0.0001 & 0.0001 & 0.0001 & 0.0001 & 10 & 10 & 10 & 10 \end{bmatrix}).$$

Again R_α is a 8×8 matrix.

Bibliography

[1] M. Vanin, "Modeling, identification and navigation of autonomous air vehicles", 2013.

[2] M.Dempsey, "Eys of the army-u.s army roadmap for unmanned aircraft systems", 2010-2035, 2010.

[3] K. Fregene, "Unmanned aerial vehicles and control", lockheed martin advanced technology laboratories, Control Systems, IEEE , vol. 32, no. 5, pp. 32-34, 2012, issn: 1066-033X. doi: 10.1109/MSC.2012.2205474.

[4] S. Bouabdallah, A. Noth and R. Siegwart, "PID vs LQ Control Techniques Applied to an Indoor Micro Quadrotor", Proc. of 2004 IEEE/RSJ Int. Conference on Intelligent Robots and Systems, September 28 - October 2, Sendai, Japan, 2004.

[5] T. Madani and A. Benallegue, "Control of a quadrotor mini-helicopter via full state backstepping technique", Proc. of the 45th IEEE Conference on Decision and Control, pp. 1515-1520, 2006.

[6] T. Madani and A. Benallegue, "Backstepping sliding mode control applied to a miniature quadrotor flying robot", Proc. of IEEE Industrial Electronics, the 32nd Annual Conference, pp. 700- 705, 2006.

[7]] H. Voos, "Nonlinear control of a quadrotor micro-UAV using feedback-linearization", In Proc. of the 2009 IEEE International Conference on Mechatronics, Malaga, Spain, April 2009.

[8] A. Benallugue, A. Mokhtari, L. Fridman, "High-order Sliding-mode Observer for a Quadrotor UAV", International Journal of Robust and Nonlinear Control, Vol 18, Issue 4-5, pp. 427-440, 2008.

[9] C. Coza and C. J. B. Macnab, "A new robust adaptive-fuzzy control method applied to quadrotor helicopter stabilization", NAFIPS Annual meeting of the North American Fuzzy Information Society, pp. 454-458, 2006.

[10] Raffo, Guilherme V., Manuel G. Ortega, and Francisco R. Rubio. "Backstepping/nonlinear H_∞ control for path tracking of a quadrotor unmanned aerial vehicle", American Control Conference IEEE, 2008.

[11] F. Senkul and E. Altu, "Modeling and Control of a Novel Tilt-Roll Rotor Quadrotor UAV", Proc. of IEEE International Conference on Unmanned Aircraft Systems (ICUAS'13), Atlanta USA, pp. 1071-1076, 28-31 May 2013.

[12] A. Sanchez, J. Escareno, O. Garcia, and R. Lozano, "Autonomous hovering of a noncyclic tiltrotor UAV: Modeling control and implementation", Proc. of the 17th IFAC Wold Congress 2008, pp. 803-808.

[13] S. Salazar-Cruz, R. Lozano, J. Escaren, "Stabilization and nonlinear control for a novel trirotor mini-aircraft", Control Engineering Practice 17(2009) 886-894.

[14] J. Escareno, A. Sanchez, O. Garcia, R. Lozano, "Triple Tilting Rotor mini-UAV: Modelling and Embedded Control of the Attitude", 2008 American Control Conference Westin Seattle Hotel, Seattle, Washington, USA June 11-13, 2008.

[15] J. Wu, H. Peng, Q. Chen, X. Peng, "Modeling and control approach to a distinctive quadrotor helicopter", ISA Transactions 53(2014) 173-185.

[16] F. Senkul, E.Altug, "Modeling and Control of a Novel Tilt-Roll Rotor Quadrotor UAV", 2013 International Conference on Unmanned Aircraft Systems (ICUAS).

[17] H. Romero, S. Salazar-Cruz, A. Sanchez and R. Lozano, "A New UAV Configuration Having Eight Rotors: Dynamical Model and Real-Time Control", 46th IEEE Conference on Decision and Control December, 2007.

[18] C. Micheli, "Design, identication and control of a tiltrotor quadcopter UAV", Master Thesis, Politecnico di Milano, 2016.

[19] R. Murray, Z. Li, and S. Sastry, "A Mathematical Introduction to Robotic Manipulation", 1994, CRC.

[20] K. P. Valavanis, Ed., "Advances in Unmanned Aerial Vehicles: State of the Art and the Road to Autonomy", New York, NY, USA: Springer-Verlag, 2007.

[21] C.-T. Chen, "Linear System Theory and Design", 1999, Oxford Univ. Press.

[22] M. Cutler , N. K. Ure , B. Michini and J. P. How, "Comparison of fixed and variable pitch actuators for agile quadrotors", Proc. AIAA Guid., Navig. Control Conf., pp. 1-17, 2011.

[23] M. Ryll, H. H. Bulthoff and P. R. Giordano, "A novel overactuated quadrotor unmanned aerial vehicle: Modeling, control, and experimental validation", IEEE Trans. Control Syst. Technol., vol. 23, no. 2, pp. 540-556, 2015.

[24] R. Scattolini, L. Magni, "Advanced and multivariable control", Pitagora, 2014.

[25] D. Pal, "Design of Quadratic Optimal Regulator for DC Motor", International Journal of Research and Discovery (IJRD) Volume: 1, Issue: 1, June 2016.

[26] B. N. Datta, "Numerical Methods for Linear Control Systems: Design and Analysis", 2004, Elsevier.

[27] K. Zhou and J. C. Doyle, "Essentials of Robust Control", 1998, Prentice-Hall.

List of Figures

List of Tables